

Standard Test Methods for: “Nondestructive and Localized Determination of Stress-Strain Curve and Initiation Fracture Toughness of Ferritic Steel Samples and Structures Using Haggag Tensile and Toughness Method (HTTM)”

Copyright 1988-2015, Fahmy M. Haggag, ABI Services, LLC, Oak Ridge, TN, USA.

1. Scope of the Test Method

- 1.1. The Haggag Tensile and Toughness Method (HTTM), known also as the Automated Ball Indentation^{®1} (ABI[®]), covers the determination of the true-stress versus true-plastic-strain curve and initiation fracture toughness of metallic materials and structural components using the automated ball indentation (ABI) test technique. It can be used for any metallic material with thickness greater than 0.5 mm (0.02 in). It requires a surface that is smooth and that has a minimum distance of 0.5 mm (0.02 in) between free edges. The ABI test method can be performed using a laboratory bench-top instrument or a portable field device.
- 1.2. The HTTM is in compliance with ASTM Standard E636-14 and Report L52280 of the Pipeline Research Council International (PRCI). A 3-minute and a 6-minute videos of two ABI tests conducted in the field and in the lab are available from: <http://abiservices-usa.com/videos/>. The HTTM has been in successful commercial use in twenty countries since 1989.
- 1.3. The ABI test can be conducted at a wide range of sample temperatures. Current experience has shown to perform well at ranges between -196 and 816°C (-320 to 1500°F). Testing at higher temperatures can be performed provided that the test surface is not severely altered by oxidation or corrosion during the test.
- 1.4. The purpose of the ABI test method is to determine tensile properties (including true-stress versus true-plastic-strain curve, yield strength, uniform ductility, strain-hardening exponent, ultimate strength, and Lüders strain), and fracture toughness as a nondestructive and localized alternative to the five (5) destructive test methods conducted according to ASTM standards E 8, E 21, E 646, E1820, and E1920.
- 1.5. The ABI test determines the initiation fracture toughness of ferritic steel samples and structures at various test temperatures.
- 1.6. *This standard does not purport to address all the safety concerns, if any, associated with its use. It is the responsibility of the user to establish appropriate safety and health practices and determine the applicability of regulatory limitations prior to use.*

2. Referenced Documents

2.1. ASTM Standards:

- E 4 Practices for Force Verification of Testing Machines
- E 6 Terminology Relating to Methods of Mechanical Testing
- E 8 Test Methods for Tension Testing of Metallic Materials
- E 21 Test Methods for Elevated Temperature Tension Tests of Metallic Materials
- E 74 Practice for Calibration of Force Measuring Instruments for Verifying the Force Indication of Testing Machines

¹ Automated Ball Indentation[®] and ABI[®] are registered trademarks owned by Fahmy M. Haggag, Oak Ridge, Tennessee, USA and are used with permission.

E 646 Test Methods for Tensile Strain-Hardening Exponents (n -Values) of Metallic Sheet Materials

E1820 Test Methods for Fracture Toughness

E1920 Test Method for Determination of Reference Temperature, T_0 , for Ferritic Steels in the Transition Range

3. Terminology

- 3.1. *Definitions*— The definitions of terms relating to tension testing appearing in Terminology E 6 shall be considered as applying to the terms used in these test methods of automated ball indentation (ABI) testing. Additional and new terms related to this standard are defined as follows:
- 3.1.1 *Force-depth partial unloading slope* [FL^{-1}]*—*the ratio of spherical indentation force to indentation depth increment during the upper 50% unloading.
- 3.1.2 *Meyer's index, m* *—*a material constant related to the strain hardening of the metal.
- 3.1.3 *Yield parameter (A)* [FL^{-2}]*—*a test material parameter related to the yield strength and strain hardening of the metal that expresses the resistance of metal to penetration by a spherical indenter.
- 3.1.4 *Material's yield slope (β_m)**—*a material type constant related to the yield strength of each class of metal (e.g., aluminum, ferritic steel, stainless steel, titanium, uranium alloys, etc.).
NOTE--It is an empirical value similar to the 0.2% offset value of the yield strength as defined in the uniaxial tension test.
- 3.1.5 *ABI-derived yield strength (σ_y)* [FL^{-2}]*—*an ABI parameter that is related to the 0.2% offset yield strength from tension tests of most metallic materials.
- 3.1.6 *Constraint factor (α_m)**—*a material constant related to the resistance of metal to plastic spherical deformation within a specific range of strain rate or indenter speed.
- 3.1.7 *Effective ball indentation strain rate ($\dot{\epsilon}$)**—*the average strain rate from all indentation cycles performed at a single test location during a complete ABI test.
NOTE--The ball indenter strain rate ($\dot{\epsilon}$) for each cycle is the ratio of indenter velocity (v) to the indentation chordal diameter (d_i) multiplied by 0.4 ($\dot{\epsilon} = 0.4 v/d_i$).
- 3.1.8 *Strain-hardening exponent (n)**—*the exponent in the empirical relationship between true-stress (σ_t) and true-plastic-strain (ϵ_p), $\sigma_t = K\epsilon_p^n$.
NOTE--It is computed as the slope of the E 646 assumed linear relationship between logarithm true-stress and logarithm true-plastic-strain.
- 3.1.9 *Strength coefficient (K)* [FL^{-2}]*—*an experimental constant, computed from the fit of the data to the assumed power law (described in E 646) that is numerically equal to the extrapolated value of true stress at a true-plastic-strain value of 1.00.
- 3.1.10 *Discontinuous yielding or Lüders strain (ϵ_L)**—*in a uniaxial tension test, a hesitation or fluctuation of force, such as is sometimes observed at or near the onset of plastic deformation, due to localized yielding (The stress-strain curve need not appear to be discontinuous.)
NOTE-- In an ABI test the Lüders strain behavior is manifested in the material pile-up around the indentation. In an ABI test Lüders strain is calculated from its relationship with the material yield strength, strain-hardening exponent, and strength coefficient.

4. Summary of Test Methods

- 4.1 A spherical (ball) indenter is forced into the surface of a metallic sample or a structural component. The spherical shape of the indenter causes an increasing strain with increased indentation depth up to a maximum of 0.2 or 20% true-plastic-strain. A true strain of 20% corresponds to a penetration depth equal to the indenter radius. The penetration depth of the spherical indenter into the test surface is measured with a displacement transducer such as a spring-loaded linear variable differential transformer (LVDT). The current strain produced is a function of the penetration depth. The force required to indent the material to increased depth values is measured with a force transducer such as a load cell. The current stress at any time is a function of the current indentation force. Periodic partial unloadings during the test are used to determine the elastic strain. The elastic strain is subtracted from the total strain to give the plastic strain. The incremental values of the ABI-measured true-stress and true-plastic-strain are calculated from the indentation force-depth data (based on elasticity and plasticity theories) and plotted to form a true-stress versus true-plastic-strain curve of the material. The ABI-derived yield strength is determined from the force-depth data. Other properties, including the strain-hardening exponent (n), strength coefficient (K), Lüders strain (ϵ_L), uniform ductility, and ultimate strength (UTS), may also be estimated from the ABI test. Also, the ABI test can be performed without intermediate partial unloadings (i.e., in a single cycle of continuous loading up to the desired maximum indentation depth/strain followed by complete unloading). This approach is preferred for high temperature or high strain rate testing to avoid indentation creep and nonlinear unloading slopes, respectively. The single cycle ABI test produces a curve of true-stress versus true-strain (i.e., total true strain since the elastic strain component cannot be subtracted due to the elimination of partial unloadings).
- 4.2 The entire test is fully automated (computer-controlled) where the spherical indenter is driven into the test surface at a desired speed which controls the strain rate of the ABI test, and the indentation force versus penetration depth are continuously collected (using a 16-bit resolution data acquisition system or better) during the entire test.
- 4.3 For laboratory specimens, the test samples can be cooled or heated to the desired ABI test temperature using an environmental chamber to bring both test sample and indenter to the desired test temperature while the force and displacement transducers are kept outside the chamber. When the depth sensor is positioned outside the environmental chamber the compliance of the testing machine shall be considered. A temperature-resistant LVDT or a clip gage can be used inside the environmental chamber. Testing at higher temperatures can be performed provided that the test surface is not severely oxidized (e.g., by utilizing an inert gas or a vacuum chamber). The test sample and the indenter shall maintain test temperature within $\pm 2.0^\circ\text{C}$ ($\pm 4^\circ\text{F}$) before conducting and during the entire ABI test.

5. Significance and Use

- 5.1 The stress-strain curve measured with the ABI test has been demonstrated to correlate with the stress-strain curve measured in a tension test. The localized ABI test is nondestructive and can be used in-situ to measure the stress-strain properties of a material sample or of a component part in service. Therefore, it can be used to measure stress-strain properties where insufficient material is available to use in a destructive tension test. The ABI test leaves a shallow spherical depression on the test surface with no sharp edges (hence, no crack initiation sites). Furthermore, it leaves a favorable compressive residual stress at the test site (similar to shot peening but on a slightly larger scale). The ABI test is also useful in testing small volumes of welds and irregularly shaped heat-affected-zones (HAZs).

- 5.2 The ABI test is particularly useful where a life extension evaluation is planned for a component and adequate materials property data are not available. Also, it can be used to measure properties for materials that may have service damage that has caused a change in tensile properties during service life (e.g. neutron embrittlement of nuclear pressure vessels). Another important application is the determination of yield strength of ferritic steel components, such as oil and gas pipelines, when no documentation exists for the original and/or repair material and when a deterministic fitness-for-service evaluation is required for safe operation at current or higher (up-rated) pressures.
- 5.3 The ABI test is a macroscopic/bulk technique that measures the properties on a small volume of material. This capability is valuable in mapping out property gradients in welds and HAZs. The minimum diameter of the indenter must be large enough such that the spherical indentation, produced at the smallest practical depth/strain, covers at least three grains of the metallic sample. This requirement is the same for the minimum thickness of a tensile specimen in order to measure macroscopic/bulk properties. The ABI technique can be used to measure the stress-strain properties of a material that may have a sharp gradient of mechanical properties. This, for example, exists in a weldment where the base metal and the weld metal have different strength and ductility and the HAZ may have a very sharp gradient of properties. Here the ABI test can measure the flow properties (true-stress versus true-plastic-strain curve) of a small volume of material and can measure the strength profile along a line traversing from one base metal through the HAZ, the weld metal and continuing through the other base metal.
- 5.4 Although the ABI test is nondestructive, the strain-hardening exponent (n) determined from the test is a function of the uniform plastic strain of many metallic materials with a power-law true-stress versus true-plastic-strain curve (e.g. nuclear pressure vessels and carbon steel materials).
- 5.5 Although there is no necking (similar to that occurring at maximum force in a tension test), the uniform ductility and ultimate tensile strength are determined from the plot of true-stress versus engineering strain.
- 5.6 The value of Lüders strain (an important property for evaluating steel sheet metals in automotive industry) is calculated from the ABI-measured yield strength, strain-hardening exponent, and strength coefficient.

6. Apparatus

- 6.1 *Testing Machines*—Machines used for ABI testing on metal samples or structures shall conform to the requirements of Practices E 4 for force verification of testing machines. The choice of bench-top or field-testing machine type depends on the application.
- 6.2 The forces used in determining the true-stress versus true-plastic-strain curve from an ABI test with a certain diameter indenter shall be within the verified loading range of the testing machine as defined in Practices E4 (Standard Practices for Force Verification of Testing Machines). The maximum ABI force depends on the indenter diameter, maximum indentation depth, and the flow properties of the metal test sample or structure. The force transducer capacity should be appropriate for the indenter diameter and the test material flow properties. The non-linearity and non-repeatability of the force transducer shall not exceed $\pm 0.1\%$ and $\pm 0.03\%$ of the full scale (maximum capacity) of the load cell, respectively. The accuracy of the force transducer shall be within $\pm 1\%$ of the full working range. The temporary attachment method (e.g., manual or electric magnets, V-blocks with mechanical clamps, etc.) shall ensure: (a) perpendicularity of the indenter axis to the test surface, and (b) enough pull force to counter the maximum indentation push force plus the weight of the load frame of the portable testing machine. The minimum components of the testing machine include a rigid load frame suitable for bench-top or field applications (for metal component testing), a driving mechanism (such as an electric motor and a mechanical actuator), an appropriate capacity force transducer such as a load cell, a gripping device for holding the indenter, a bracket for holding the displacement transducer (e.g., a spring-loaded

Linear Variable Differential Transformer “LVDT”), a high resolution 16-bit data acquisition card or better, and a computer (either a desk-top or a laptop) with appropriate software and interface to the data acquisition card and the motor to provide complete control of the ABI test as well as post-test data analysis. The complete automation of the testing machine shall provide closed loop operation with continuous measurement and software limits on both the force and depth signals. The software limits prevent possible damage to the force or depth sensors and avoid violating the depth requirement for a valid ABI test.

- 6.3 *Indentation depth measurement and calibration*—a high-resolution depth sensor with a full range not greater than 1.0 mm (such as a spring-loaded LVDT) is used for ABI testing. The non-linearity of the depth sensor shall be less than 0.20% of the full range output, and the non-repeatability shall be less than 0.00010 mm (0.000004 in). The depth sensor is mounted on a bracket attached to the indenter holder. The accuracy of the depth sensor shall be within $\pm 1\%$ of the full working range. The depth sensor is calibrated using a micrometer or a similar device with an accuracy of 0.001 mm.
- 6.4 *Indenters*—The spherical indenter shall be polished and free of surface defects. The tolerance shall be ± 0.003 mm or better in any diameter of the indenter. Spherical indenters made from either tungsten carbide or silicon nitride where the spherical tip and the indenter stem are manufactured from the same material are used for ABI testing of metal samples and structural components. Spherical indenters with various diameters (e.g., 0.254-mm, 0.508-mm, 0.762-mm, and 1.575-mm with a deviation from these values of not more than 0.003 mm in any diameter) can be used for ABI testing depending on the test volume available and the grain size of the test metal. The tungsten carbide indenter shall have an elastic modulus at room temperature greater than 620 GPa and Vickers hardness not less than 1500. Silicon nitride indenters, with Vickers hardness of 1600 or higher and an elastic modulus at room temperature greater than 320 GPa, are recommended for use at test temperatures above 400°C and up to 1000°C. The indenter holder, such as a stainless steel chuck, should provide easy interchangeability of indenters, solid support of the indenter stem, and ensure the perpendicularity of the indenter tip to the test surface. The indenter diameter is selected based on the test volume (thickness, final indentation depth, and available test area) and the grain size of the metal. Whenever possible the largest size indenter is selected to increase the test volume and to increase precision. Small indenters such as the 0.254-mm diameter require very smooth surface finish using at least 600-grit polishing. The maximum indentation depth shall not exceed 10% of the specimen thickness, and the indentation chordal diameter shall be enclosed within the desired test material including small welds or HAZ. Appropriate force transducer capacity should be used for each size indenter for increased resolution (e.g., 4.45 kN, 1.11 kN, 445 N, and 222 N load cells are appropriate for indenter diameters of 1.575-mm, 0.762-mm, 0.508-mm, and 0.254-mm, respectively).
- 6.5 *Load-frame attachments for field-testing of pipelines and pressure vessels*—Various attachment methods can be used to temporarily attach the load frame of the portable/field testing machine to structural metal components. These attachments (e.g., manual or electric magnets for magnetic components such as carbon steel pipelines and pressure vessels, V-blocks with mechanical clamps for non-magnetic materials) shall ensure: (a) perpendicularity of the indenter to the test surface, and (b) enough pull force to counter the maximum indentation push force plus the weight of the load frame of the portable testing machine.
- 6.6 *Furnaces or Heating Devices*—When performing an ABI test on a specimen at elevated temperature, the furnace or heating device used shall be capable of maintaining a uniform temperature of the entire test specimen and the indenter so that variation of not more than $\pm 2.0^\circ\text{C}$ ($\pm 4^\circ\text{F}$) for temperatures up to and including 427°C (800°F) occurs. Heating by self-resistance is not accepted.

7. Specimen/Structural Preparation

Surface finish and optional sample mounting—The ABI test location shall have a smooth machined/ground surface, or if necessary, it shall be polished to a surface finish of 1.6 μm (63 micro-inches). Care shall be taken in surface preparation to avoid overheating or cold working the surface. An irregular or very small sample shall be mounted in Bakelite or a similar hard material with the top and bottom surfaces parallel. A rigid swivel sample holder shall be used if the mounted sample does not have parallel surfaces. The ABI test area of a metal component shall be polished locally using hand held equipment. Other component areas must be prepared properly for the attachments used (e.g., any rust must be removed from carbon steel pipelines in order for the magnetic attachments to secure the load frame of the portable machine to the pipeline test location). When indentations are made on a curved surface, the minimum radius of curvature of the surface shall be not less than 25 times the diameter of the ball indenter.

8. Test Procedures

- 8.1 *Objective and Overview*—The overall objective of the test methods is to develop ABI force-depth curves that can be used to calculate the ABI-derived yield strength, true-stress versus true-plastic-strain curve, strain-hardening exponent, strength coefficient, uniform ductility, and ABI-estimated ultimate strength. Two procedures can be used: (1) a multi-cycle ABI test with intermediate partial unloadings or (2) a single-cycle ABI test with no intermediate partial unloadings.
- 8.2 *Locating indentation positions*—The planar spacing of indentations shall be at least three diameters from their centers and within at least two diameters from free edges.
- 8.3 *Initial test preload*—An initial test preload is required for calculating the zero indentation point, on the ABI force-depth curve, at which the ball indenter contacts the test surface for the first time. A small indentation preload (less than 10% of the indentation force at a depth value of 30% of the indenter radius), appropriate to the indenter diameter, is applied to the sample or structure before the continuation of the ABI test. Minimum suggested preloads for the four indenter diameters of 0.254-mm, 0.508-mm, 0.762-mm, and 1.575-mm are 2 N, 5 N, 10 N, and 30 N, respectively). After the preload application, the depth transducer value, indicated on the computer screen, must be small enough to ensure that there is enough remaining range of depth measurement to complete the test up to the user-specified final indentation depth. Immediately after the application of the preload, the ABI test is continued according to either the Multi-Cycle or the Single-Cycle procedures described in 8.3 and 8.4, respectively.
- 8.4 *Multi-Cycle ABI test*—The procedure involves progressive loading of the ball indenter into the test surface up to a final depth/strain (e.g., 30% of the indenter radius relates to approximately 15% strain). A minimum of five cycles shall be performed at a single ABI test location with equal increments of indentation depth. All intermediate cycles include partial unloading of the indenter (by a determined percentage of 30 –50% of the maximum cycle-force depending on the data acquisition rate). The specimen is fully unloaded at the end of the test. All indentation loading and unloading are performed with a constant indenter speed during the entire ABI test. The force-depth data is collected (using a 16-bit data acquisition system or better) and displayed in real-time on the computer screen during the complete ABI test. The ABI test is fully computer controlled with closed-loop software limits on both force and depth data. If during the test any limit is reached, the loading process is immediately halted and the test area is unloaded. The unloading slopes are linear because of the elastic recovery of the test volume. These slopes are not parallel and increase with increasing indentation depth as the deformation volume increases while the sample elastic modulus does not change with indentation depth. Fig.1 shows a schematic of cyclic loading and unloading of a ball indenter into the surface of test material:

- (a) Schematic of applied force versus indentation depth, (b) Indentation geometry during force application and after force removal (complete unloading).
- 8.5 *Single-Cycle ABI Test*—The ABI test can be performed without intermediate partial unloadings (i.e., in a single cycle of continuous loading up to the desired maximum indentation depth/strain followed by complete unloading). This approach is preferred for high temperature or high strain rate testing to avoid indentation creep and nonlinear unloading slopes, respectively. The single cycle ABI test produces a curve of true-stress versus true-strain (i.e., total true strain since the elastic strain component cannot be subtracted due to the elimination of partial unloadings).
- 8.6 *Field Testing Precautions*—When performing ABI field tests on metallic structures at various locations the load frame of the portable testing machine shall be moved carefully between far locations to avoid possible mechanical damage to the force and depth sensors and the indenter during shipment in an automobile or airplane.
- 8.7 *Indenter Installation and Replacement*—When an indenter is changed, the new indenter shall be seated properly and fully in its stainless steel chuck holder. The indenter is seated by performing an ABI test at an additional test location and verifying that there is no indenter slippage inside its chuck holder (i.e., there is no horizontal force-depth behavior on the real-time force-depth display on the computer monitor).

9. Calculation of Results

- 9.1 *Calculation of indentation depth associated with initial test preload*—Linear regression is performed on the force-depth data of the best linear part of the first loading cycle in a Multiple-Cycle ABI test or from the early part (first 5%) of the force-depth curve in a Single-Cycle ABI test. The intersection of the extrapolation of the linear regression fit with the X-axis determines the depth value associated with the preload value. Hence, this indentation depth value is added as a correction or adjustment to all depth data of the raw force-depth curve previously collected with temporarily assuming a zero depth associated with the preload value as shown in Fig. 2. This adjustment results in a lateral shift of the raw force-depth curve to the right by the amount determined from the data regression shown in Fig. 3. The corrected/adjusted ABI force-depth data is shown in Fig. 4.

NOTE 1--The force-depth curve of an ABI test is linear because of the effect of the strain hardening behavior of metallic materials on the shape of the force-depth curve. A nonlinear/ball indenter produces increasing strain values with increasing depth while a linear indenter (Vickers, cone, etc.) produces a single value of strain regardless of depth and a nonlinear (concave) force-depth curve. Hence, a stress-strain curve can be produced only using a nonlinear indenter. ABI test results on many materials in various conditions are reported in References 1 through 16.

- 9.2 *Calculation of the plastic-depth associated with each cycle in a Multi-Cycle ABI test*—Linear regression analysis is performed on the data of each elastic partial unloading, and the calculated slope is extrapolated where its intersection with the depth axis determines the plastic depth associated with the upper force of the cycle. This is shown schematically in Fig. 1a and graphically (from an example ABI test data using a 0.762-mm diameter indenter) in Fig. 5.
- 9.3 *Calculation of true-stress and true-plastic-strain pairs*—The incremental values of the true-stress versus true-plastic-strain curve are calculated from Equations 1 through 11(3). For a single-cycle ABI test, the plastic chordal diameter is replaced by the total chordal diameter (calculated from the total depth, Equation 9). It is important to note that these equations are independent of the work-hardening behavior of the material (i.e., regardless if it follows a power law or not). The value of the constraint factor index (α_m) used in equation 6 depends on the class of material, and the test strain rate. It is determined empirically from comparison of true-stress versus true-plastic-strain curves from ABI and tension tests (values for carbon steel and

aluminum alloys are given in Appendix X1). For an unknown material, a value of 1.1 should be used in Equation 6 for the constraint factor index.

- 9.4 *Calculation of the ABI-derived yield strength*—The yield strength determined from an ABI test is calculated from Equations 9 through 11 (3). Figure 6 is an example plot of Equation 10. The values of the material's yield slope (β_m) and the yield strength offset-constant (B) depend on the class of metal and the indenter diameter (slope and offset-constant values for carbon steel and aluminum alloys are given in Appendix X1). These values are empirically determined to be in close agreement with the 0.2% offset yield strength determined from uniaxial tension tests (16, 17). For example, a recommended value for the yield strength slope (β_m) for carbon steel testing using a 0.762-mm tungsten carbide indenter is 0.22. The values of the yield parameter (A), material's yield slope (β_m), and yield strength offset-constant (B) used in the ABI-derived yield strength calculation shall be documented in the ABI test report. For an unknown material, values of 0.20 and 0.00 should be used for the material yield strength slope and yield strength offset-constant, respectively.
- 9.5 *Calculation of strain-hardening exponent (n), strength coefficient (K), Lüders strain (ϵ_L), and estimated ultimate strength (UTS)*—The true-stress versus true-plastic-strain results from the ABI test are fitted to the power law form of Equation 12 as described in Method E 646. A single power curve is fitted to the entire curve between yield and the final true strain at the end of the test, or the yield strength point can be eliminated from the data fit, depending on the desired strain range for determining the “ n ” value. The strain-hardening exponent (n) and the strength coefficient (K) are determined from this empirical representation of the flow curve (Equation 12). An example of ABI-measured flow properties, including the yield strength value, and their power-law fitting is shown in Fig. 7. The Lüders strain is calculated from Equation 13. If the flow properties of the test material are well represented by the power law form of Equation 12 (E 646), then the ultimate strength can be estimated from Equation 14. If the ABI-measured true-stress versus true-plastic-strain curve does not follow a single power law, then it shall be calculated from the plot of true-stress versus engineering strain as explained in item 9.6 below and in Figure 8.

NOTE 2—In the ABI test there is no necking behavior similar to that occurring in a tension test. Hence the UTS can be estimated from Equation 14 or it can be calculated using the plot of true-stress versus engineering strain.

- 9.6 *Calculation of uniform ductility and ultimate tensile strength (UTS)*—A straight line is drawn from an engineering strain value of -1.00 to be a tangent to the true-stress versus engineering strain curve (18). The X-axis value of this line at the tangent intersection point determines the uniform ductility while the intersection of the line with the Y-axis, at the origin (0,0), determines the engineering UTS value. An example of the calculation of the Uniform Ductility and the Engineering UTS from the ABI-measured True-Stress versus Engineering Strain curve is shown in Figure 8.
- 9.7 *Indenter Diameter Selection and Data Qualification*—The indenter diameter is selected based on the test volume (thickness, final indentation depth, and available test area) and the grain size of the metal. For a Single-Cycle test, some of the force-depth data collected at very low depth (the first 5% depth of the entire test) shall be excluded from the stress-strain curve calculations if the indentation chordal diameter at such a small depth covers less than three grains. Notice that the progressive ball indentation at lowest practical depth increment should cover more than three grains in order to obtain macroscopic stress-strain properties. An example comparison between a small indentation (made using a 0.254-mm diameter indenter and a force of 2 N) and the grain size of the test material is provided in Figure 9. An example of qualified ABI force-depth data (generated using a 0.508-mm diameter indenter), test results, and comparison with tensile test

results are shown in Fig. 10. An example of the geometry of a large indenter (1.575-mm diameter) is shown also in Figure 10 (inset photo).

$$\text{Where:} \quad \epsilon_p = \frac{0.2d_p}{D} \quad (1)$$

ϵ_p = true plastic strain,
 d_p = plastic indentation diameter,
 D = diameter of the ball indenter.

$$\text{Where:} \quad \sigma_t = \frac{4P}{\pi d_p^2 \delta} \quad (2)$$

σ_t = true stress,
 P = applied indentation force,
 δ = a parameter whose value depends on the stage of development of the plastic zone beneath the indenter as shown in Equation 5 below.

$$d_p = \left\{ 0.5CD \left[\frac{h_p^2 + \left(\frac{d_p}{2} \right)^2}{h_p^2 + \left(\frac{d_p}{2} \right)^2 - h_p D} \right] \right\}^{1/3} \quad (3)$$

Where h_p is the plastic indentation depth and “C” is defined in Equation 4 below.

$$C = 5.47P \left(\frac{1}{E_1} + \frac{1}{E_2} \right) \quad (4)$$

Where E_1 and E_2 are the elastic moduli of the indenter and the test sample, respectively.

$$\delta = \begin{cases} 1.12 & \Phi \leq 1 \\ 1.12 + \tau \ln \Phi & 1 < \Phi \leq 27 \\ \delta_{\max} & \Phi > 27 \end{cases} \quad (5)$$

$$\delta_{\max} = 2.87\alpha_m \quad (6)$$

Where α_m is the constraint factor index.

$$\Phi = \frac{\epsilon_p E_2}{0.43\sigma_t} \quad (7)$$

$$\tau = \frac{\delta_{\max} - 1.12}{\ln(27)} \quad (8)$$

Where “ \ln ” is the natural logarithm.

$$d_t = 2\sqrt{h_t D - h_t^2} \quad (9)$$

Where h_t and d_t are the total indentation depth and total indentation diameter while the force is being applied, respectively.

$$\frac{P}{d_t^2} = A \left(\frac{d_t}{D} \right)^{m-2} \quad (10)$$

Where A is the material yield parameter and m is Meyer's index.

$$\sigma_y = \beta_m * A + B \quad (11)$$

Where σ_y is the ABI-determined yield strength, β_m is the material yield slope, and B is the yield-strength offset-constant.

$$\sigma_t = K \epsilon_p^n \quad (12)$$

Where K is the strength coefficient and n is the strain-hardening exponent.

$$\ln \left(\frac{K}{\sigma_y} \right) = \epsilon_L - n * \ln \epsilon_L \quad (13)$$

Where ϵ_L is Lüders strain.

$$UTS = K \left(\frac{n}{e} \right)^n \quad (14)$$

Where UTS is the ABI-estimated ultimate strength and $e = 2.718$.

10. Report

A recommended format for reporting the test parameters, equipment parameters, analysis parameters, and test results for both Multi-Cycle and Single-Cycle ABI tests is shown in Fig. 11 (a) while an additional reporting format suggested for the Multi-Cycle ABI test only is shown in Fig. 11(b).

Report the following information for each ABI test: test name, test material and test number, test atmosphere, test temperature, indenter diameter, indenter speed, number of unloadings, data acquisition rate, percentage of the partial unloading, maximum indentation depth (percentage of indenter radius used in final indentation), indenter material and its elastic modulus, constraint factor, yield strength slope and offset, total number of data points collected, reporting of any force or depth limits triggered during the ABI test, ABI results of ABI-derived yield strength, strain-hardening exponent, strength coefficient, ABI-estimated engineering UTS , ABI-calculated engineering UTS (from the plot of true-stress versus engineering strain), and calculated uniform ductility.

Report the additional data and test results for each cycle of a Multi-Cycle ABI test: cycle number, maximum total depth, plastic depth, maximum force, plastic indentation chordal diameter, unloading slope, R^2 value (regression coefficient) for the regression analysis of the partial unloading slope, total chordal diameter, true-plastic-strain, and true-stress.

Report the following graphs: force-depth data before and after adjustment for the depth associated with the applied preload, yield strength calculation plot, true-stress versus true-plastic-strain curve with individual points and power-law fit, and a plot of the true-stress versus engineering strain.

11. Precisions and Bias

- 11.1 *Precision*—The precision of any of the various ABI-determined flow properties cited in these test methods is a function of the precision and bias of the various measurements of indenter diameter, the precision and bias of the depth measurement, the precision and bias of the force measurement, and the precision and bias of the data acquisition system used to construct the force-depth curve. It is not possible to make meaningful statements concerning the precision and bias for all these measurements. However it is possible to derive useful information concerning the precision of the ABI-measured flow properties in a global sense from interlaboratory test programs. Values of the ABI-determined yield strength and true-stress versus true-plastic-strain curves were evaluated in (15) for several pressure vessel steels at various test temperatures. The ABI-derived yield strength and estimated ultimate strength values were evaluated in (16) for seven pipeline steels, with various grades and manufacturing dates, tested at room temperature using two indenter diameters (0.508 mm and 0.762 mm), and the ABI test results were compared to the results from tensile tests on the same materials. An interlaboratory test program² gave the following values for the coefficients of variation for the most commonly ABI-measured flow properties:

	Coefficient of Variation, %				
	ABI-Yield Strength	ABI-Estimated Ultimate Strength	Strength Coefficient	Strain-Hardening Exponent	Uniform Ductility
CV % _r	1.4	1.5	2.6	5.8	6.9
CV % _R	1.7	2.3	3.4	6.7	7.8

CV %_r = repeatability coefficient of variation in percent within a laboratory

CV %_R = repeatability coefficient of variation in percent between laboratories

- 11.1.1 The values shown are the averages from five ABI tests on each of four frequently tested metals (ferrous and non-ferrous), selected to include most of the normal range for each property listed above. Twenty ABI tests were conducted by each of six different laboratories using commercial Stress-Strain Microprobe (SSM) systems³ especially designed for ABI testing. The slightly higher coefficients of variation for the strain-hardening exponent and the uniform ductility are due to the fact that these two properties depend on the shape of the stress-strain curve and the homogeneity of the metal. The values of the coefficient of variation are provided to allow potential users of these test methods to assess, in general terms, their usefulness for a proposed application. Additional precision statistics are provided in Appendix X1.

- 11.2 *Bias*—The procedures in the ABI test methods for measuring flow properties have no bias because these properties can be defined only in terms of the test methods. When comparing flow properties from ABI and tension tests the agreement will be closer for those tests conducted at the same strain rate. Flow properties from ABI tests may not correlate with results from uniaxial tension tests conducted on materials that exhibit different behavior under tension or compression loading, such as those fabricated from powder compacts. The ABI test results will be closer to those from compression tests on powder compacts.

² Supporting data are available from ABI Services, LLC: e-mail: info@abiservices-usa.com. Request Report ATC-RR-ABI-2003.

³ ABI Services, LLC, Oak Ridge, TN 37830, USA, website: www.abiservices-usa.com is the source of bench-top and field instruments for ABI testing. Stress-Strain Microprobe® is a registered trademark owned by Fahmy M. Haggag and is used with permission.

12. Calibration and Standardization

12.1 The following devices should be calibrated against standards traced to national standards (in the United States, National Institute of Standards and Technology). Applicable ASTM methods are listed beside the device.

Force-measuring system	E 4 and E 74
Micrometers (for calibrating the depth sensor)	

12.2 Calibrations should be as frequent as is necessary to assure that the errors in all tests do not exceed the permissible variations listed in these test methods. The maximum period between calibrations of the force and depth sensors shall be 18 months.

13. Verification of Testing Machines

13.1 New testing machines shall be verified once prior to service use by conducting at least one ABI test on the end tab of each flat tensile specimen manufactured in triplicates from two alloys of two types of metallic materials (e.g. steels and aluminums) with a wide range of yield strength values for each material type (e.g., 200 to 700 MPa). The new machine is accepted if the following two conditions are met: (a) the average estimated yield strength from each triplicate ABI tests is within $\pm 10\%$ of the average yield strength measured from the triplicate tension tests, of each of the four alloys tested according to ASTM Standard E8, and (b) the average value of the final plastic indentation diameter, d_p , measured in two perpendicular directions shall be within $\pm 5\%$ of the corresponding value calculated using Equation 3 for each of the ABI tests conducted on the four alloys. The comparison of the optical versus calculated values of the final plastic indentation diameter is an indirect verification of the overall performance of the testing machine, including its force transducer, depth sensor, and ball indenter diameter and perpendicularity to the test surface.

13.2 Periodic verification is conducted according to the user's requirements and application with a minimum frequency of once per year by performing at least three ABI tests on the end tabs of three flat tensile specimens manufactured from a Ferritic steel material with yield strength greater than 500 MPa. The average value of the estimated yield strength from the ABI tests shall be within $\pm 10\%$ of the average measured yield strength from tension tests conducted according to ASTM Standard E8. Due to the possibility of damage during handling, it is strongly recommended that portable ABI testing machines be verified every day that they are used. Both lab and portable testing machines shall have a minimum verification of once per year.

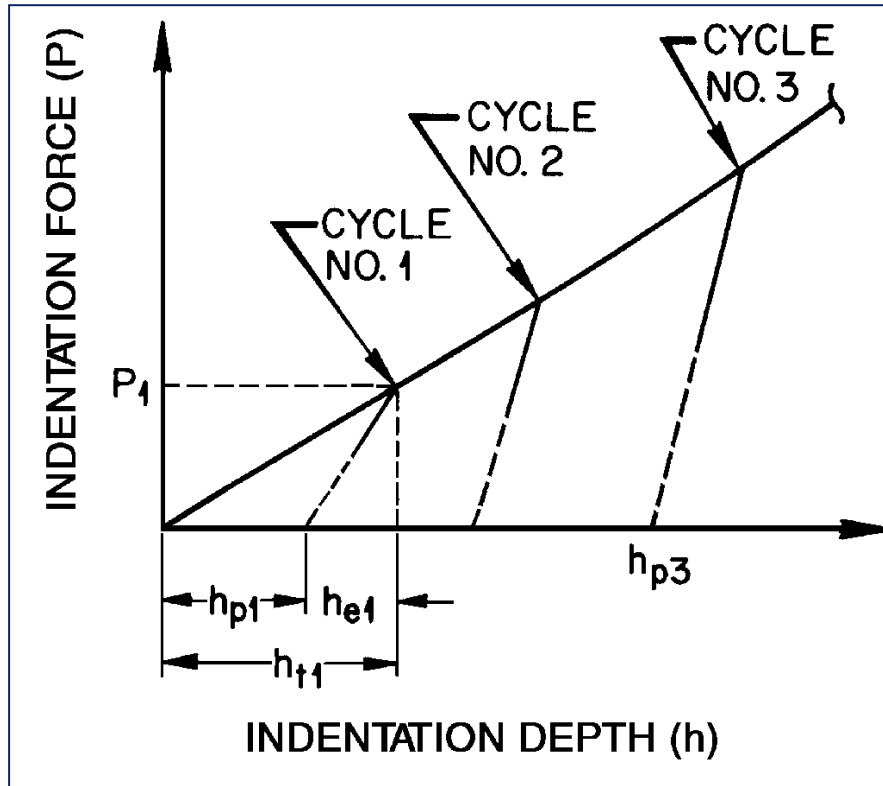
14. Keywords

14.1 Automated Ball Indentation, ball indenter, indenter velocity, force-depth data, partial unloading slope, yield parameter, yield strength, true-stress, true-plastic-strain, strain-hardening exponent, strength coefficient, ultimate strength, uniform ductility, Lüders strain

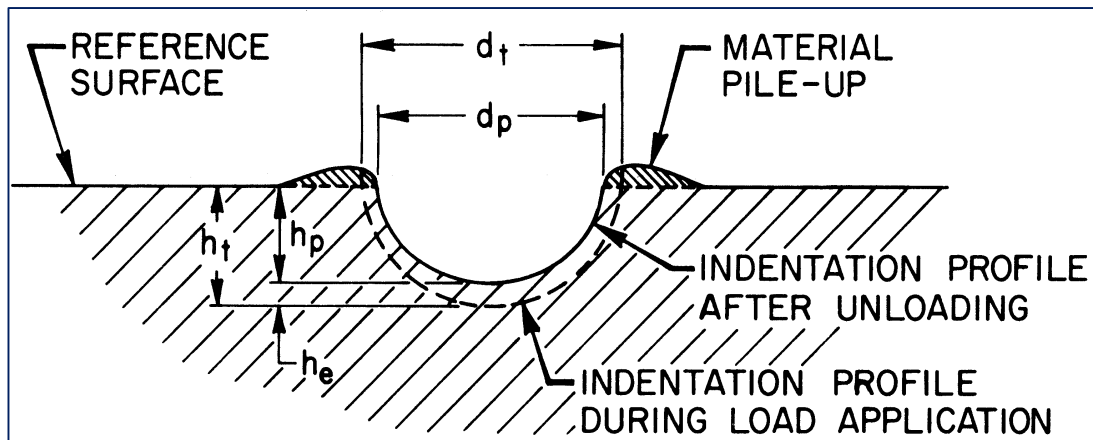
REFERENCES

(1) Haggag, F. M., "Field Indentation Microprobe for Structural Integrity Evaluation," U.S. Patent No. 4,852,397, August 1, 1989.

- (2) Haggag, F. M., et al., "Use of Portable/In Situ Stress-strain Microprobe System to Measure Stress-Strain Behavior and Damage in Metallic Materials and Structures," *ASTM STP 1318*, 1997, pp. 85-98.
- (3) Haggag, F. M., "In-Situ Measurements of Mechanical Properties Using Novel Automated Ball Indentation System," *ASTM STP 1204*, 1993, pp. 27-44.
- (4) Haggag, F. M., et al., "Use of Automated Ball Indentation Testing to Measure Flow Properties and Estimate Fracture Toughness in Metallic Materials," *ASTM STP 1092*, 1990, pp. 188-208.
- (5) Byun, T. S., et al. "Measurement of Through-the-Thickness Variations of Mechanical Properties in SA508 Gr.3 Pressure Vessel Steels Using Ball Indentation Test Technique," *International Journal of Pressure Vessels and Piping*, Vol. 74, 1997, pp. 231-238.
- (6) Haggag, F. M., et al., "A Novel Stress-Strain Microprobe for Nondestructive Evaluation of Mechanical Properties of Materials", *Nondestructive Evaluation and Materials Properties III*, The Minerals, Metals & Materials Society, 1997, pp. 101-106.
- (7) Haggag, F. M., et al., "Using Portable/In-Situ Stress-Strain Microprobe System to Measure Mechanical Properties of Steel Bridges During Service," SPIE Proceedings on "Nondestructive Evaluation of Bridges and Highways," Vol. 2946, 1996, pp. 65-75.
- (8) Haggag, F. M., et al., "Nondestructive Detection and Assessment of Damage in Aging Aircraft Using a Novel Stress-Strain Microprobe System", SPIE Proceedings on "Nondestructive Evaluation of Aging Aircraft, Airports, and Aerospace Hardware," Vol. 2945, 1996, pp. 217-228.
- (9) Haggag, F. M. et al., "Characterization of Strain-Rate Sensitivity of Sn-5%Sb Solder Using ABI Testing," *Microstructures and Mechanical Properties of Aging Materials II*, TMS, 1995, pp. 37-44.
- (10) Haggag, F. M., et al., "Application of Flow Properties Microprobe to Evaluate Gradients in Weldment Properties," *International Trends in Welding Sciences and Technology*, ASM, 1993, pp. 629-635.
- (11) Haggag, F. M., et al., "Measurement of Yield Strength and Flow Properties in Spot Welds and Their HAZs at Various Strain Rates," *International Trends in Welding Sciences and Technology*, ASM, 1993, pp. 637-642.
- (12) Haggag, F. M. et al., "Structural Integrity Evaluation Based on an Innovative Field Indentation Microprobe," *ASME PVP-Vol. 170*, 1989, pp. 101-107.
- (13) Haggag, F.M., et al., "The Use of Field Indentation Microprobe in Measuring Mechanical Properties of Welds," *Recent Trends in Welding Science and Technology*, TWR'89, ASM, 1990, pp. 843-849.
- (14) Druce, S. G., et al., "The Use of Miniature Specimen Techniques for the Assessment of Material Condition," *ASME PVP-Vol. 252*, 1993, pp. 58-59.
- (15) Haggag, F. M., *Nondestructive and Localized Measurements of Stress-Strain Curves and Fracture Toughness of Ferritic Steels at Various Temperatures Using Innovative Stress-Strain Microprobe™ Technology*, DOE/ER/82115-2, October 1999.
- (16) Haggag, F. M., *Nondestructive Determination of Yield Strength and Stress-Strain Curves of In-Service Transmission Pipelines Using Innovative Stress-Strain Microprobe™ Technology*, ATC/DOT/990901, September 1999.
- (17) Haggag, F. M., *In-Situ Measurement of Pipeline Mechanical Properties Using Stress-Strain Microprobe – Validation of Data for Increased Confidence & Accuracy*, PRCI Report Number L52280, April 2007.
- (18) Dieter, George E., *Mechanical Metallurgy*, Second Edition, McGraw-Hill Book Company, 1976, p. 344.



(a)



(b)

Fig. 1 Cyclic Loading and unloading of a ball indenter into the surface of test material: (a) Schematic of applied force versus indentation depth, (b) Indentation geometry during force application and after force removal (complete unloading).

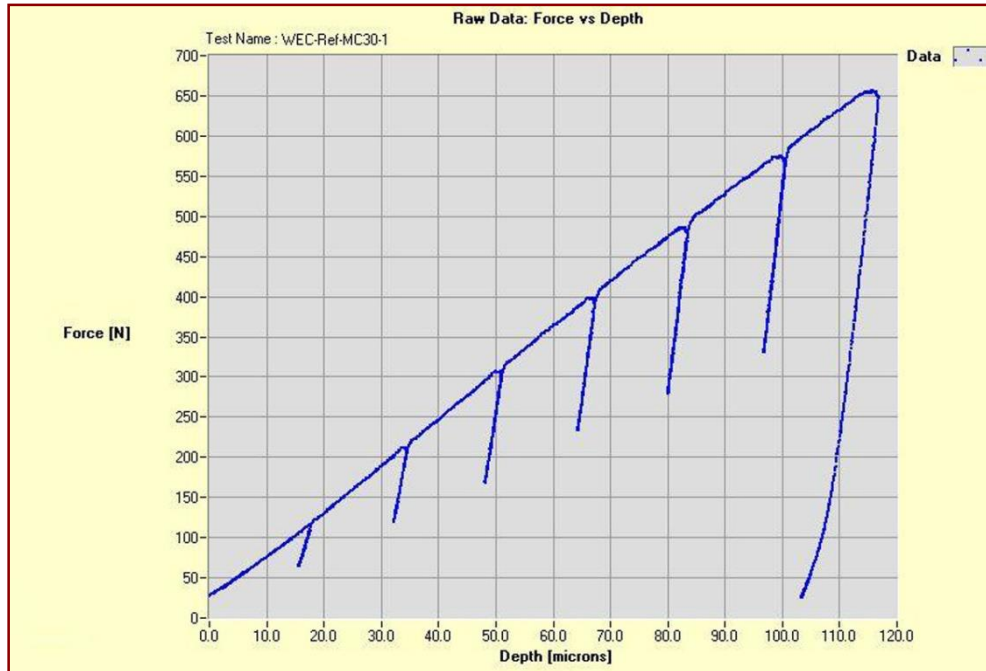


Fig. 2 Example of raw data collected using a 0.762-mm diameter tungsten carbide indenter on a ferritic steel sample. Note that a zero value is temporarily assumed for the indentation depth associated with the preload value of the ABI test. The actual indentation depth value associated with the preload value is calculated next in Fig. 3.

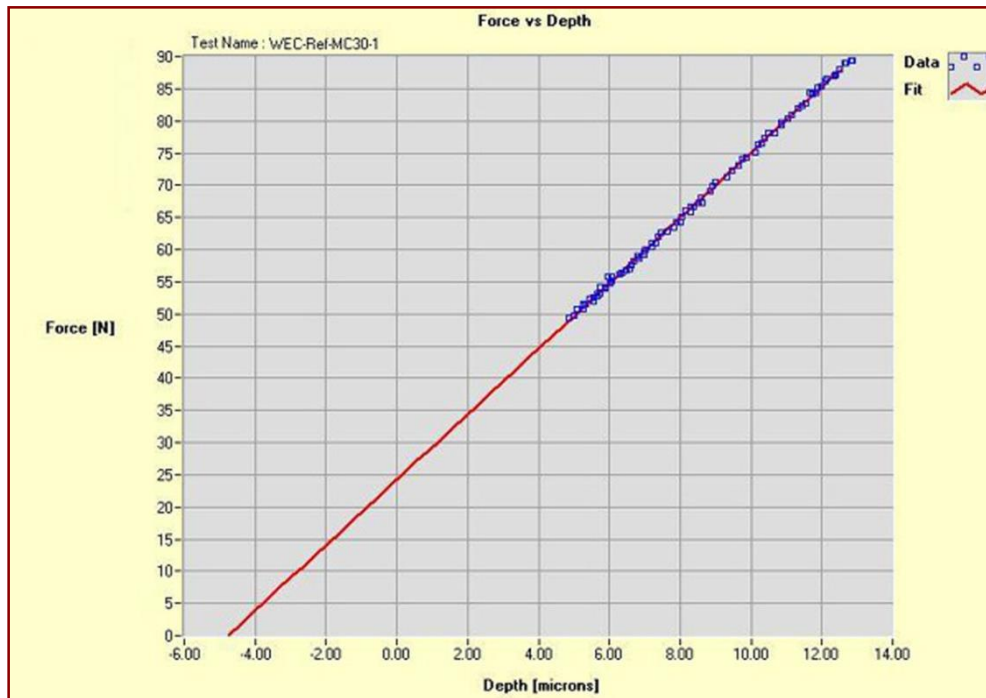


Fig. 3 Example of the linear regression of the force-depth data from the first loading cycle of the Multi-Cycle ABI test shown in Fig. 2. The solid line resulting from the linear regression is used to calculate the indentation depth associated with the indentation preload value (the intersection value of the X-axis).

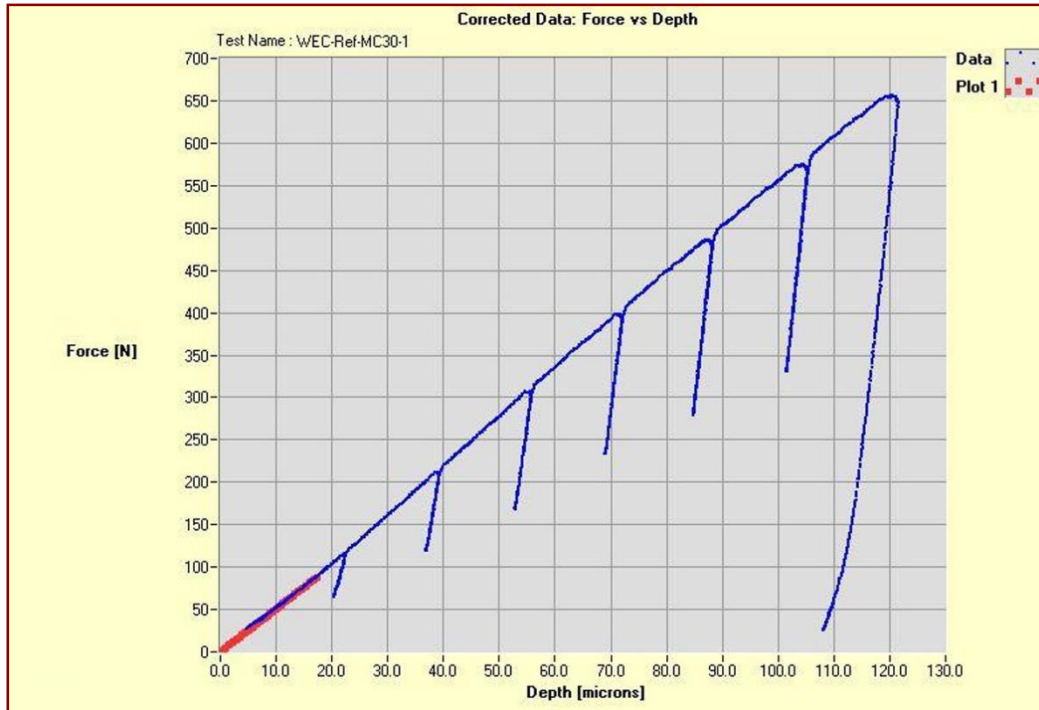


Fig. 4 Example of the corrected ABI data (after shifting the curve to the right by the amount of indentation depth associated with the indentation preload calculated in Fig. 3).

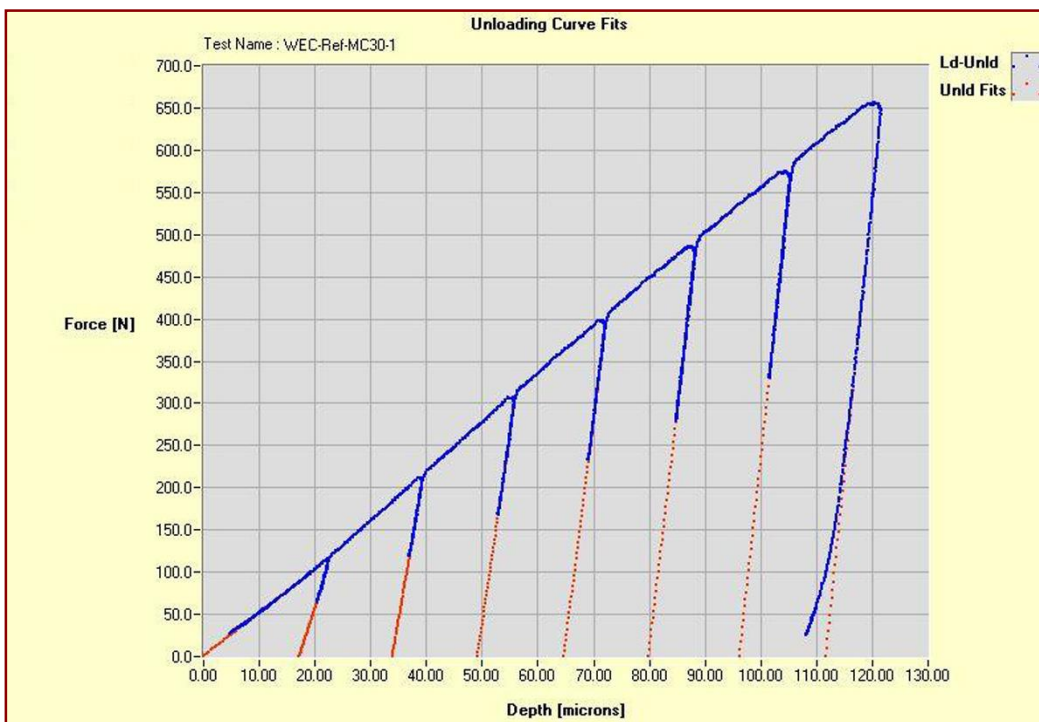


Fig. 5 Example of the corrected force-depth data showing the linear regression of the elastic unloadings (dotted lines). The intersection of the dotted lines (extrapolated from the unloadings) with the X-axis determines the plastic-depth associated with each cycle.

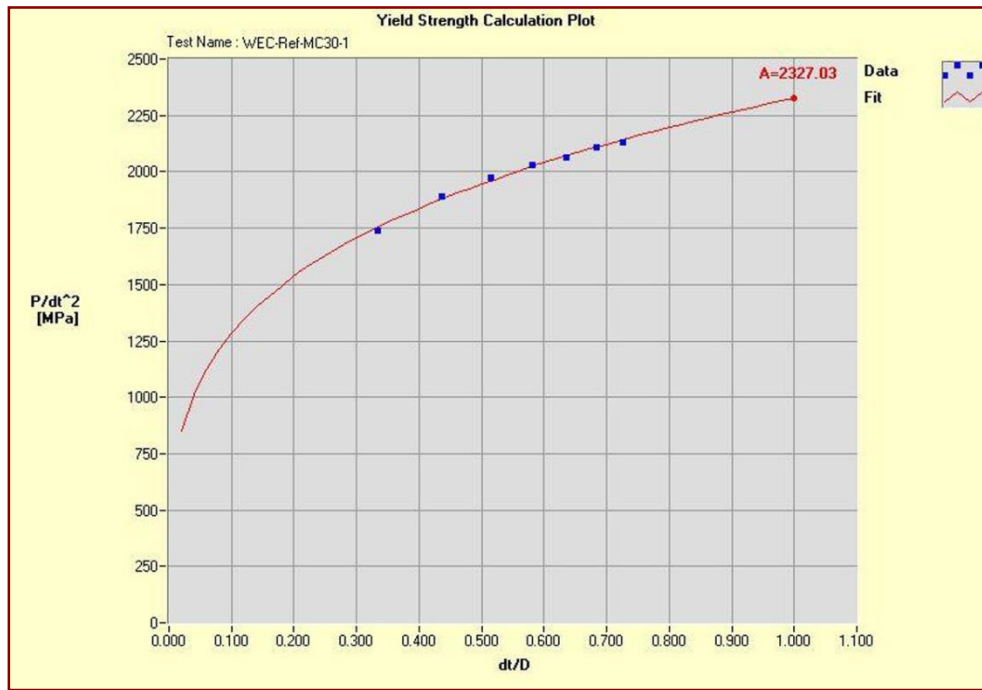


Fig. 6 Yield strength calculation plot. The extrapolation of the curve to an X-axis value of 1.00 produces the yield strength parameter “A” that is used in Equation (11) to calculate the yield strength value.

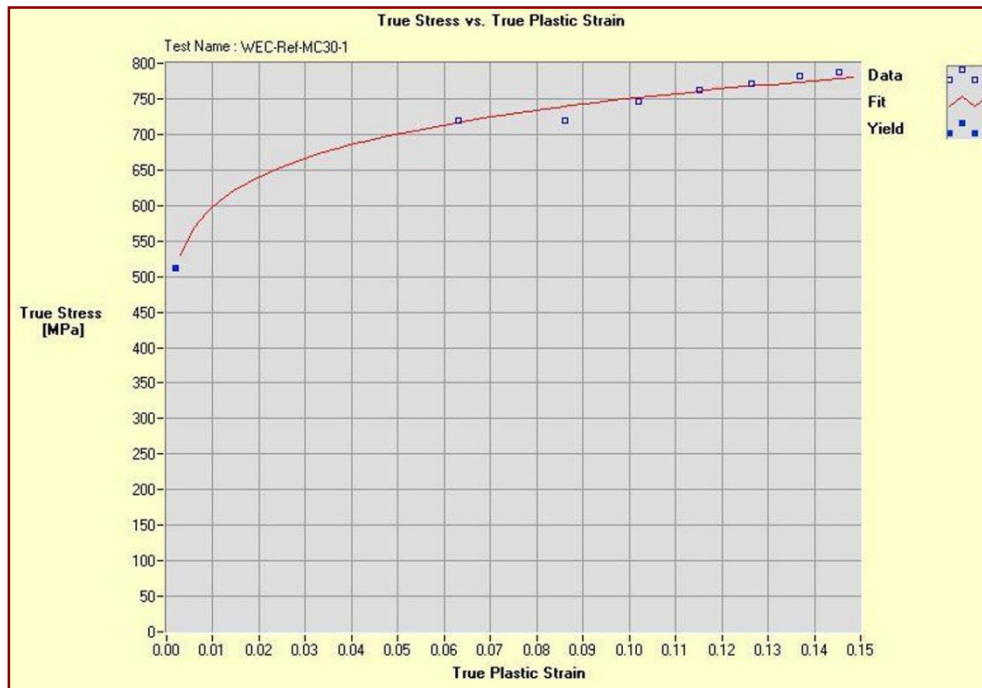


Fig. 7 Example of the true-stress versus true-plastic-strain curve determined from the ABI test. The yield strength is plotted with a different symbol (a solid square instead of an open square) since it is calculated from the plot of Fig. 6 and it is not a back-extrapolation from the other points. The solid line is calculated from the power-law fitting of the data as described in ASTM Standard E 646.

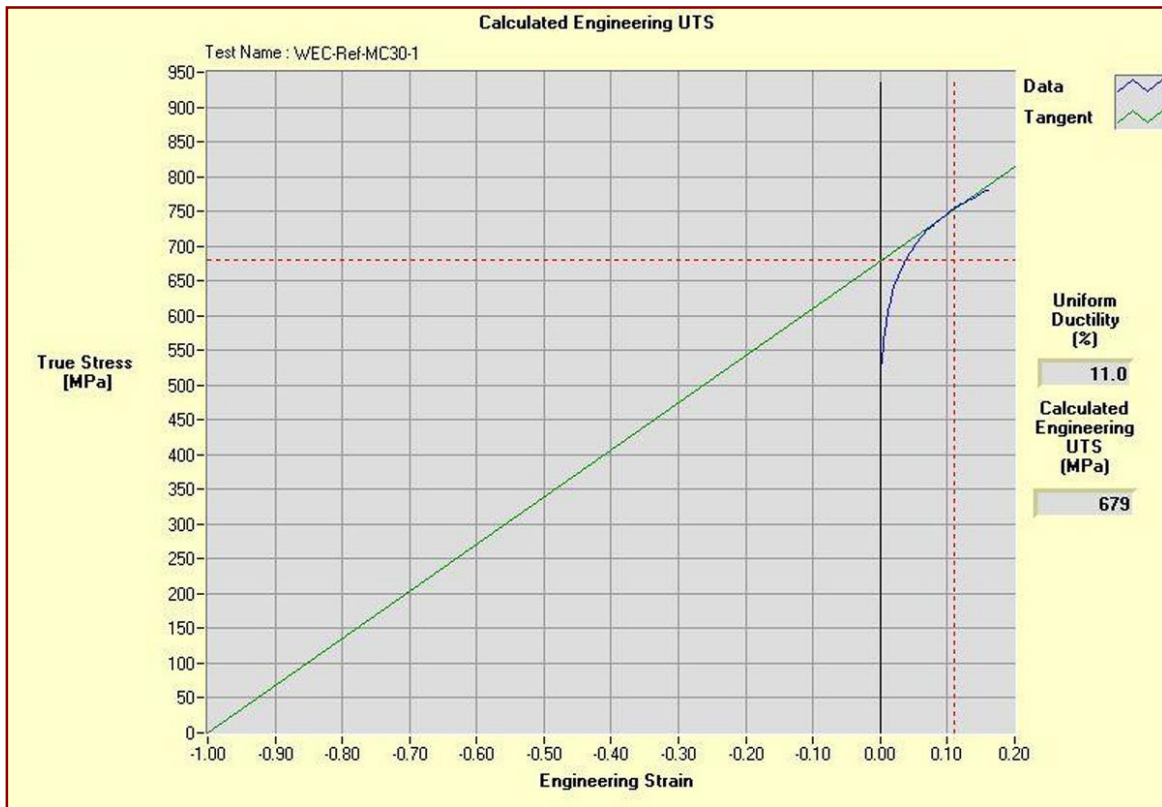


Fig. 8 Example of the calculation of the Uniform Ductility and the Engineering Ultimate Strength (*UTS*) from the ABI-measured True-Stress versus Engineering Strain curve.

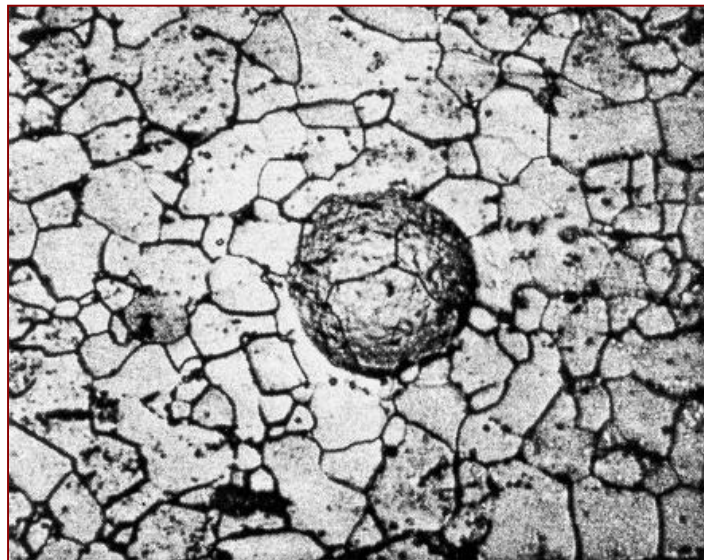


Fig. 9 Spherical indent in 1015 steel (20 μm grain size) obtained at a force of 2 N using a 254 μm (0.010 in) diameter indenter. Notice that the progressive ball indentation at lowest depth increment should cover more than three grains in order to obtain macroscopic stress-strain properties.

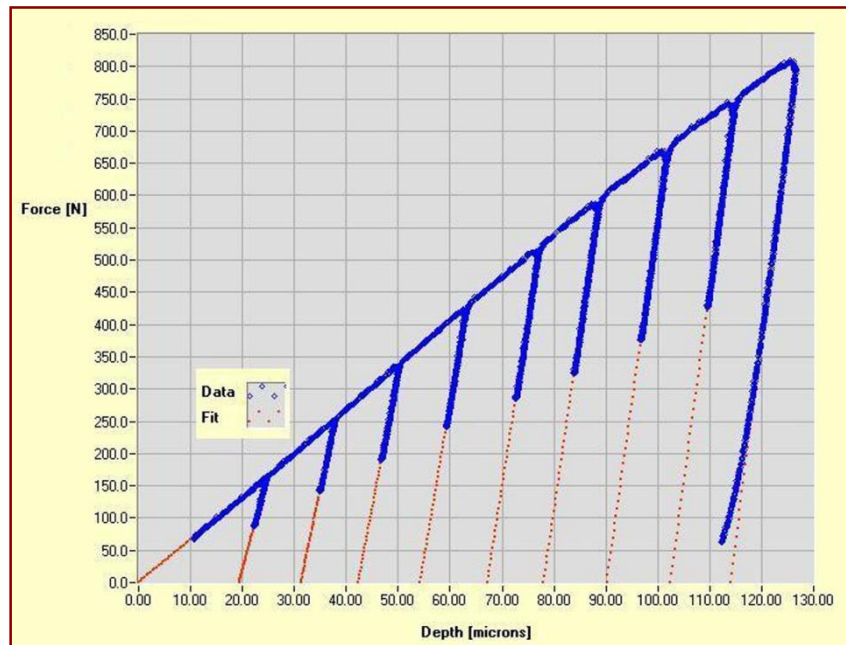


Fig. 10 (a) Indentation force versus depth in an ABI test using a 0.762-mm (0.030-in) diameter tungsten carbide indenter on a ferritic steel material.

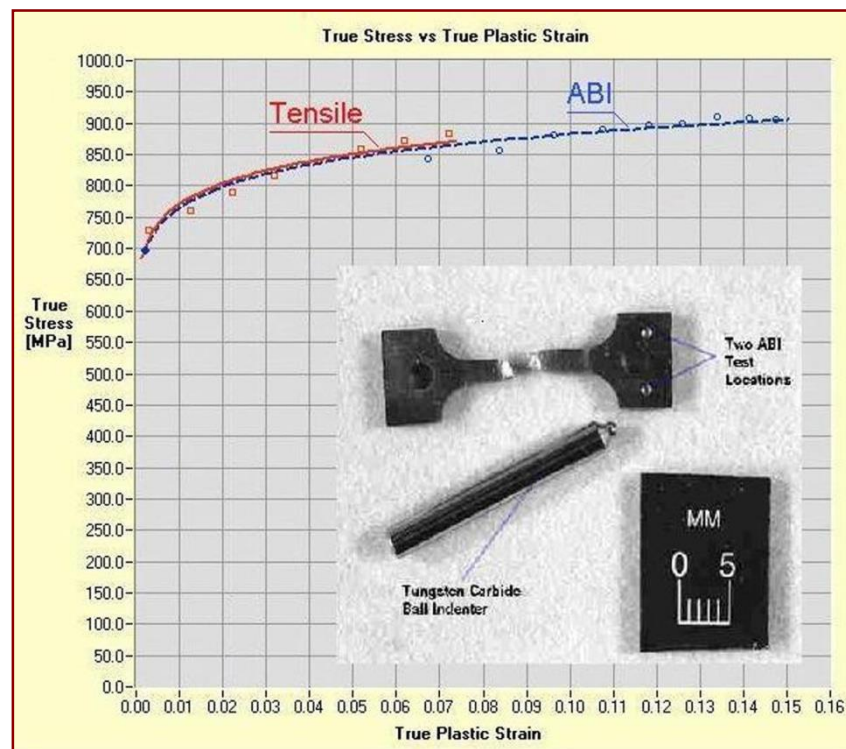


Fig. 10 (b) True-stress versus true-plastic-strain curves from ABI (using a 0.762-mm diameter indenter, data shown in Fig. 10a) and tension tests on a ferritic steel. A miniature tensile specimen is shown in the inset photo with two indentations made with a larger indenter (1.575-mm diameter).

Test Name: WEC-Ref-MC30-1		Test Date: Tuesday, March 20, 2001 4:35 PM	
Project ID:		Operator: Tom	
Material & Test No.: WEC Block, Test No.1			
Additional Info.:			

TEST PARAMETERS		ANALYSIS PARAMETERS	
Atmosphere:	Air	Ind. Material:	Tungsten Carbide
Temperature:	22 [C]	Ind. Modulus:	641.22 [GPa]
Indenter Speed:	0.010 [mm/sec]	Sample Modulus:	206.84 [GPa]
Indenter Diameter:	0.7620 [mm]	Initial Ld Levels:	Top: 89.50 [N] Bot: 49.42 [N]
No. of Unloadings:	7	Regression Fit:	Top: 30.0% Bot: 0.0%
Acquisition Rate:	50 [pts/sec]	Constraint Factor Index(α):	1.2000
% Unloading:	40.00	Material Yield Slope(β):	0.2200
Pre-Load Set Point:	22.241 [N]	Material Yield Offset(B):	0 [MPa]
Indenter Rad. Used:	30.0 [%]		

EQUIPMENT PARAMETERS		RESULTS	
LVDT Slope:	0.05 [mm/V]	No. of Data Pts.:	3375
LVDT Offset:	0.00 [mm]	Abort Data Pt.:	0
LVDT CutOff Depth Lim:	0.13 [mm]	End Message:	Normal
Load Cell Slope:	446.60 [N/V]	Ld./Depth Slope:	5.09 [kn/mm]
Load Cell Offset:	0.00 [N]	Pre-Ld. Depth:	-4.75 [mic]
Load Cell Cutoff Limit:	1067.57 [N]	Pre-Ld. Force:	26.39 [N]
Load Cell Zero Reading:	51.19 [N]	Initial Ld, R ² :	0.999
Correct For Ind. Comp:	NO		

LVDT Correction:	0.00 [mm]
Inclde Yield Pt.?:	YES
Yield Level :	0.2 [%]
R ² Yield Strength:	0.995
R ² Stress-Strain:	0.992
Meyer's Number:	2.258
Yield Par., A:	2327 [MPa]
Yield Strength(A, β , B):	512 [MPa]
Strain Hard. Exp(n):	0.098
Strength Coeff.(K)	941 [MPa]
Yield Strength(n, K):	512 [MPa]
Est. Eng. UTS:	679 [MPa]
Calc. Eng. UTS :	679 [MPa]
Calc. Unif. Duct :	11.0 [%]

Fig. 11 (a) Suggested data reporting format for both Multi-Cycle and Single-Cycle ABI tests. Example of the first page of the ABI test report including the test parameters, equipment parameters, analysis parameters, and the test results.

ABI Analysis Results by Cycle														
Test Name: WEC-Ref-MC30-1				Test Date: Tuesday, March 20, 2001 4:35 PM										
Project ID:				Operator: Tom										
Material & Test No.: WEC Block, Test No.1														
Additional Info.:														
Cycle	Max Depth ht [mic]	PI Depth hp [mic]	Max Ld [N]	PI Dia dp [mic]	Pmax/dt^2 dt/D [MPa]	From Data	To Data	R^2	Slope [N/mic]	y-inter [N]	dt [mic]	True Plastic Strain	True Stress [MPa]	
Yield Strength												0.002	512.0	
1	21.724	17.227	112.0	239.944	0.333	1740.7	406	430	0.990	20.0	-345.1	253.630	0.063	719.1
2	38.204	33.932	208.9	327.723	0.436	1888.5	729	760	0.992	37.9	-1285.4	332.577	0.086	719.0
3	54.560	49.207	304.7	388.480	0.516	1973.5	1086	1125	0.991	44.6	-2194.5	392.926	0.102	746.4
4	70.869	64.719	397.2	439.118	0.581	2027.6	1490	1535	0.998	52.0	-3365.6	442.627	0.115	761.6
5	86.775	79.871	483.8	481.344	0.635	2064.2	1930	1990	0.995	55.8	-4453.9	484.118	0.126	771.9
6	103.130	96.199	573.7	520.936	0.684	2110.9	2425	2495	0.997	60.8	-5845.0	521.342	0.137	781.6
7	119.331	111.711	654.1	554.032	0.727	2132.4	2957	3039	0.998	64.4	-7199.4	553.860	0.145	787.9

Fig 11 (b) Suggested data reporting format for the Multi-Cycle ABI test. Example of the second page of the ABI test report including the tabulated values of the true-plastic-strain versus the true-stress data pairs from all cycles.

APPENDIX X1

Summary of the Interlaboratory Study (ILS) and Precision Statistics

X1.1 Because standard reference materials with certified ABI or tensile property values are not available, it is not possible to rigorously define the bias of ABI tests. However, by the use of carefully designed and controlled interlaboratory study, a reasonable definition of the precision of ABI test results can be obtained.

X1.2 An Interlaboratory test program was conducted in which five ABI tests were conducted on each of four widely differing ferrous and non-ferrous materials at each of six laboratories using commercial Stress-Strain Microprobe® (SSM) systems especially designed for ABI testing. The materials are two aluminum alloys (6061 and 7075) and two steel alloys (1018 and 4142) with a wide range of flow properties. Brazed 1.57-mm (0.062-inch) diameter tungsten carbide indenters were used in all 120 ABI tests. A summary of the ABI test and analysis parameters is included below. The indenter speed was fixed for all ABI tests in order to perform all tests at the same strain rate. The values of the yield strength slope (Beta) of 0.26 and 0.31 for the steel and aluminum samples, respectively, were determined empirically from comparisons with tensile test results in order to obtain very good agreement between the ABI-Determined yield strength and those from the empirical 0.2% offset method of the tension test. Similarly, the value of the constraint factor (Alpha) of 1.00 for both steel and aluminum materials was verified from overlays of the true-stress/true-plastic-strain curves from both the multi-axial ABI tests and the uniaxial tension tests. Although comparison of flow properties from ABI and tension tests is not the subject of this interlaboratory study, the overlay of true-stress versus true-plastic-strain curves from both types of tests produced very good agreement for all four materials as shown in Figures X1-1 and X1-2.

Test Parameters:

Indenter speed = 0.015 mm/s
Percentage indenter used = 20%
Pre-Load Set Point = 66.7 N
Number of Unloading Cycles = 10 (Equal Depth)
Unload (% of Cycle Maximum Force) = 40.0 %
Data Acquisition Rate = 200 Samples/sec
Indenter Elastic Modulus = 641.2 GPa

Analysis Parameters for Steel Samples:

Elastic Modulus = 206.8 GPa
Constraint Factor (Alpha) = 1.00
Yield Strength Slope (Beta) = 0.2600
Include Yield Parameter in Analysis = Yes

Analysis Parameters for Aluminum Samples:

Elastic Modulus = 68.9 GPa
Constraint Factor (Alpha) = 1.00
Yield Strength Slope (Beta) = 0.3100
Include Yield Parameter in Analysis = Yes

Tables X1.1-X1.5 present the precision statistics, as defined in ASTM Standard Practice E 691, for the yield strength (YS-ABI), estimated ultimate strength (UTS-ABI), strength coefficient (K-ABI), strain-hardening exponent (n-ABI), and calculated uniform ductility (UD-ABI).

TABLE X1.1 – Precision Statistics for the ABI-Determined Yield Strength (YS-ABI), MPa

NOTE 1—X is the average of the cell averages, that is, the grand mean for the test parameter,
 S_r is the repeatability standard deviation (within-laboratory precision),
 S_r/X is the repeatability coefficient of variation in %,
 S_R is the reproducibility standard deviation (between-laboratory precision),
 S_R/X is the reproducibility coefficient of variation, %,
 r is the 95% repeatability limits,
 R is the 95% reproducibility limits.
 $CV \%_r$ = repeatability coefficient of variation in percent within a laboratory
 $CV \%_R$ = repeatability coefficient of variation in percent between laboratories

Materials	Average (X)	S_r	$CV \%_r=(S_r/X)\%$	S_R	$CV \%_R=(S_R/X)\%$	r	R
Al 6061-T651	329.97	5.41	1.64	6.28	1.90	15.15	17.58
Al 7075-T651	545.73	7.11	1.30	8.00	1.47	19.90	22.41
Steel 1018	361.90	6.10	1.69	7.21	1.99	17.07	20.18
Steel 4142	721.30	7.79	1.08	9.58	1.33	21.81	26.82

Averages: **1.43** **1.67**

TABLE X1.2 – Precision Statistics for the ABI-Estimated Ultimate Strength (UTS-ABI), MPa

Materials	Average	S_r	$CV \%_r$	S_R	$CV \%_R$	r	R
Al 6061-T651	396.20	3.82	0.96	5.73	1.45	10.69	16.04
Al 7075-T651	613.03	13.76	2.24	17.23	2.81	38.52	48.25
Steel 1018	497.00	8.22	1.65	15.52	3.12	23.02	43.46
Steel 4142	1003.90	13.29	1.32	19.93	1.99	37.21	55.80

Averages: **1.54** **2.34**

TABLE X1.3 – Precision Statistics for the ABI-Determined Strength Coefficient (K-ABI), MPa

Materials	Average	S_r	$CV \%_r$	S_R	$CV \%_R$	r	R
Al 6061-T651	514.40	8.45	1.64	10.42	2.03	23.67	29.18
Al-7075-T651	768.60	29.60	3.85	36.90	4.80	82.88	103.33
Steel 1018	706.63	17.83	2.52	28.94	4.10	49.93	81.02
Steel 4142	1434.93	31.32	2.18	40.51	2.82	87.69	113.44

Averages: **2.55** **3.44**

TABLE X1.4 – Precision Statistics for the ABI-Determined Strain-Hardening Exponent (n-ABI)

Materials	Average	S _r	CV % _r	S _R	CV % _R	r	R
Al 6061-T651	0.071933	0.003764	5.23	0.004026	5.60	0.010539	0.011273
Al-7075-T651	0.058900	0.005798	9.84	0.007206	12.23	0.016234	0.020177
Steel 1018	0.109567	0.004829	4.41	0.005254	4.80	0.013520	0.014711
Steel 4142	0.111967	0.004131	3.69	0.004693	4.19	0.011567	0.013142
Averages:			5.79		6.71		

TABLE X1.5 – Precision Statistics for the ABI-Calculated Uniform Ductility (UD-ABI), %

Materials	Average	S _r	CV % _r	S _R	CV % _R	r	R
Al 6061-T651	7.41	0.88	11.88	0.98	13.22	2.47	2.74
Al 7075-T651	5.80	0.68	11.72	0.79	13.62	1.91	2.23
Steel 1018	10.35	0.23	2.22	0.25	2.42	0.64	0.69
Steel 4142	10.30	0.20	1.94	0.21	2.04	0.55	0.60
Averages:			6.94		7.83		

X1.3 In each of Tables X1.1-X1.5, the first column lists the four materials tested, the second column lists the average of the average results obtained by all laboratories, the third and fifth columns list the repeatability and reproducibility standard deviations, the fourth and six columns list the coefficient of variation for these standard deviations, and the seventh and eighth columns list the 95% repeatability and reproducibility limits.

X1.4 The averages (below columns four and six in each table) of the coefficients of variation permit a relative comparison of the repeatability (within-laboratory precision) and reproducibility (between-laboratory precision) of the ABI test parameters. This shows that the ABI-calculated uniform ductility (UD-ABI) and the ABI-determined strain-hardening exponent (n-ABI) exhibit similar but less repeatability and reproducibility than the strength measurements. The overall ranking from the least to the most repeatable and reproducible is: % ABI-calculated uniform ductility (UD-ABI), ABI-determined strain-hardening exponent (n-ABI), ABI-determined strength coefficient (K-ABI), ABI-estimated ultimate strength (UTS-ABI), and ABI-determined yield strength (YS-ABI). Note that the rankings are in the same order for the repeatability and reproducibility average coefficients of variation and that the reproducibility (between-laboratory precision) is slightly less than the repeatability (within-laboratory precision), as would be expected.

X1.5 No comments about bias can be made for this ABI interlaboratory study due to the lack of certified test results for the these specimens. However, examination of the test results from five tests each on four materials (ferrous and non-ferrous) at six laboratories showed that the ABI test methods provide excellent repeatability within a laboratory and between laboratories for the ABI-determined yield strength (YS-ABI), estimated ultimate strength (UTS-ABI), and the strength coefficient (K-ABI). The repeatability coefficients of variation for the strain-hardening exponent (n-ABI) and the uniform ductility (UD-ABI) are slightly higher because the determination of these properties depends on the shape (curvature) of the true-stress/true-plastic-strain curve and the homogeneity of the metal. The two steel materials exhibited better repeatability and reproducibility of their strain-hardening exponent and uniform ductility than the two aluminum materials because of their better homogeneity and because their flow properties (true-stress versus true-plastic-strain curves) followed a better power-law behavior.

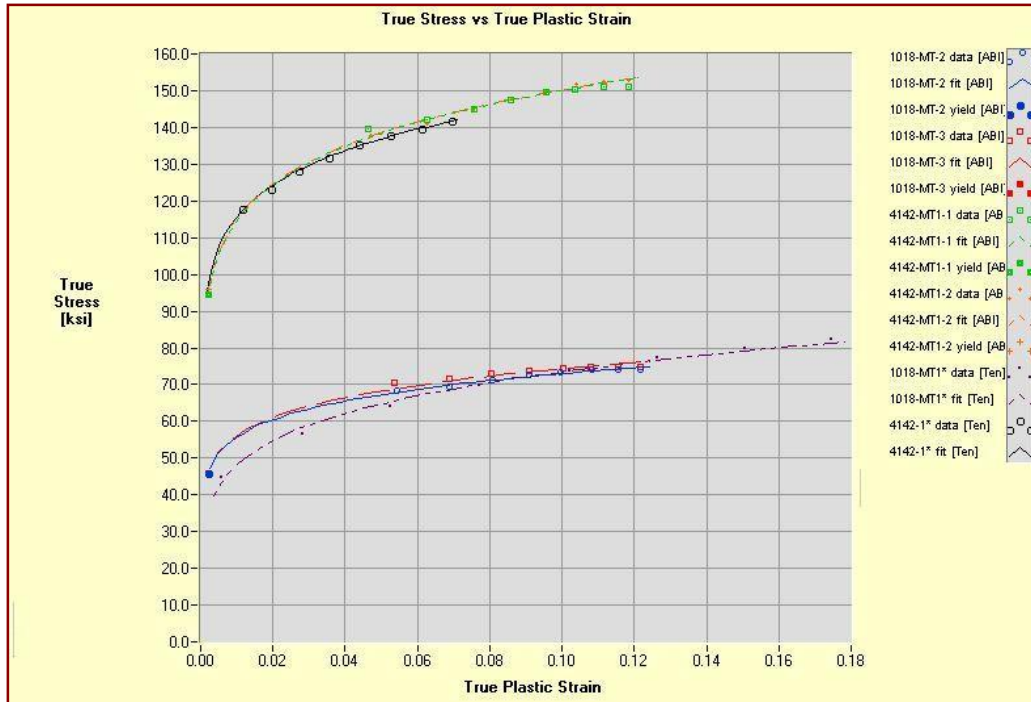


Fig. X1-1 Comparison between true-stress versus true-plastic-strain curves from ABI and tension tests of 1018 (lower curves) and 4142 steel (higher curves) samples. Two ABI tests were conducted on the end tabs of each tensile specimen.

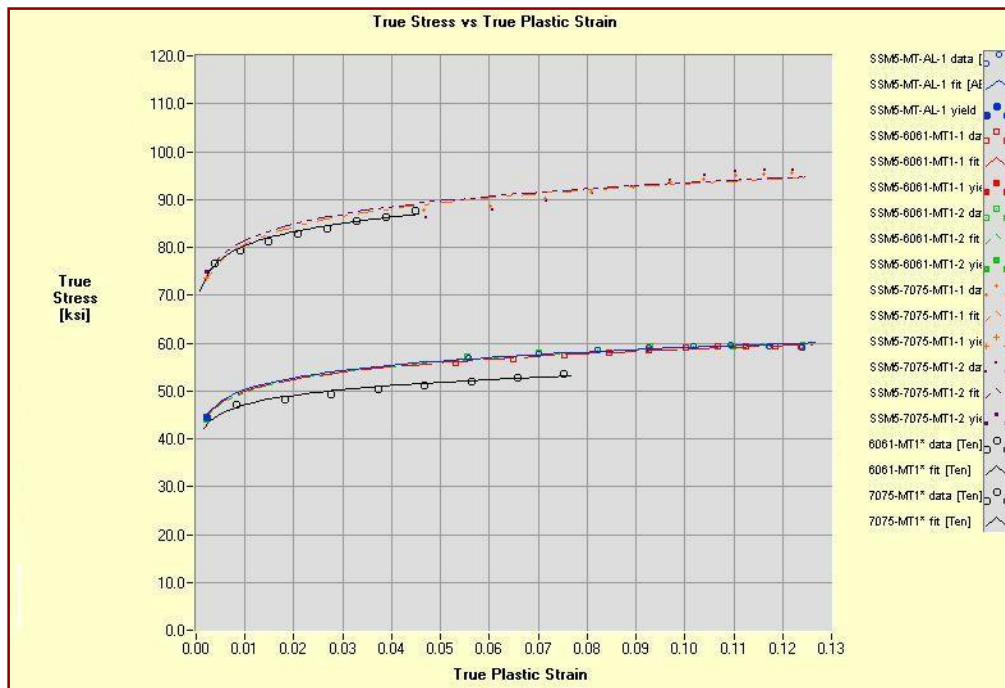


Fig. X1-2 Comparison between true-stress versus true-plastic-strain curves from ABI and tension tests of 6061 (lower curves) and 7075 aluminum (higher curves) samples. Two ABI tests were conducted on the end tabs of each tensile specimen.

Appendix X2

**Standard Haggag Tensile and Toughness Method
(HTTM), also known as ABI Test Method,
for Determining Initiation Fracture Toughness and
the Reference Temperature (T_0) of Ferritic Steels**

Appendix X2: Standard Haggag Tensile and Toughness Method (HTTM), also known as ABI Test Method, for Determining Initiation Fracture Toughness and the Reference Temperature (T_0) of Ferritic Steels

Copyright 1988-2015, Fahmy M. Haggag, ABI Services, LLC, Oak Ridge, TN, USA

X2.1 Destructive Fracture Toughness Testing

For ferritic steels (with yield strength of 275 to 825 MPa or 40-120 ksi) the fracture toughness (median value) versus temperature curve in the transition temperature region is expressed by the master curve (ASTM E-1921-97):

$$K_{Jc}(med) = 30 + 70e^{0.019(T-T_0)} \quad \text{MPa}\sqrt{\text{m}} \quad (1)$$

Where T is the test temperature and T_0 is the reference temperature when $K_{Jc} = 100 \text{ MPa}\sqrt{\text{m}}$.

In order to obtain median dynamic fracture toughness (K_{Id}) values as a function of temperature, the ASTM Standard E1921-97 equation of the static fracture toughness (K_{Jc}) master curve can be used provided that the reference temperature be shifted to a higher value that depends on the yield strength of the test material at room temperature. It is well known that the dynamic fracture toughness curve is shifted to the right hand-side of the static fracture toughness curve by a temperature shift value depending on the room-temperature yield strength of the ferritic steel material.

The median dynamic fracture toughness (K_{Id}) can be calculated from the following equation:

$$K_{Id}(med) = 30 + 70e^{0.019(T-[T_0+T_{shift}])} \quad \text{MPa}\sqrt{\text{m}} \quad (2)$$

Where T is the test temperature in $^{\circ}\text{C}$ and T_0 is the reference temperature when $K_{Jc} = 100 \text{ MPa}\sqrt{\text{m}}$. The T_{shift} can be determined from the Barsom correlation [Ref. 1] and using the average yield strength measured from multiple ABI tests at room temperature. The Barsom correlation is given by:

$$T_{shift}(^{\circ}\text{F}) = 215 - 1.5\sigma_{ys}(\text{ksi}) \quad \text{for } 36 \text{ ksi} < \sigma_{ys} < 140 \text{ ksi} \quad (3)$$

where σ_{ys} is the room-temperature yield strength of the steel material.

X2.2 Haggag Fracture Toughness Method (HFTM)

The Haggag Fracture Toughness Method (HFTM) determines the fracture toughness (K_{Jc}) value from the ABI test on ferritic steel materials by integrating the indentation deformation energy (compression of the two surfaces of the ball indenter and the test material instead of pulling two surfaces in a destructive fracture toughness test) from the beginning of the test up to a critical indentation depth. The latter is calculated using either the critical fracture stress model or the critical fracture strain model; depending on the flow properties of the material at the test temperature. The analysis first checks the attainment of the critical fracture stress (using the mean pressure plot as a function of normalized indentation depth) before a strain value of 12% or a normalized depth of 0.6. If this occurs then the test is analyzed according to this model and all ABI test results can be further analyzed using the fracture toughness master curve concept and a reference temperature is determined in order to evaluate the brittle behavior of the test material at low temperatures. If the critical fracture stress is not attained prior to a normalized depth of 0.6 then the specimen is analyzed according to the critical fracture strain model and further analysis using the fracture toughness master curve becomes invalid (or if used it will produce a very conservative

reference temperature since the test material is in the ductile temperature region instead of the transition region).

Indentation with a ball indenter generates concentrated stress (and strain) fields near and ahead of the contact of the indenter and the test surface, similar to concentrated stress fields ahead of a crack tip; albeit the indentation stress fields are mostly compressive. The high value of the stress under the ball indenter is an example of *plastic constraint* where the rigid material surrounding the indentation volume does the constraining. Hence, at a certain critical ball indentation depth, there is a high state of transverse and lateral stresses similar to those in front of a sharp notch in an elastic material. Although the conditions for crack initiation might be attained, the high degree of plastic constraint will prevent cracks from developing during ball indentation of ductile metallic materials. Therefore, only initiation fracture toughness, not tearing modulus, can be determined from ball indentation (Equations 6-12 on page 60 of Ref. 2 and shown below in Table 1). The initiation fracture toughness is calculated from the integration of the indentation deformation energy (*IDE*) up to the critical depth (when the maximum pressure underneath the ball indenter equals the critical fracture stress of the steel material at the test temperature or reaches a critical strain value of 0.12, whichever occurs first). Examples of the applications of the critical fracture stress and the critical fracture strain models from earlier ABI tests at various test temperatures are shown in Figures 1 and 2, and test results of pressure vessels and pipelines are given in References 4 through 6.

The ABI-measured fracture toughness capability is material-thickness independent since different size indenters can be used for all pipelines and pressure vessels in order to achieve valid results. Furthermore, its localized nature allows testing heat-affected-zones that cannot be tested destructively because of their irregular shapes and small volumes.

Table X2-1a – Equations (Reference X2-2)

$$\epsilon_p = \frac{0.2d_p}{D} \quad (1)$$

$$\sigma_t = \frac{4P}{\pi d_p^2 \delta} \quad (2)$$

$$d_t = 2\sqrt{h_t D - h_t^2} \quad (3)$$

$$\frac{P}{d_t^2} = A \left(\frac{d_t}{D} \right)^{m-2} \quad (4)$$

$$\sigma_y = \beta_m * A + B \quad (5)$$

$$IDE = \int_0^{h_f} P_m(h) dh = W_T \quad (6)$$

$$P_m = \frac{4P}{\pi d_t^2} \quad (7)$$

$$W = W_0 + W_T \quad (8)$$

$$(K_{Jc})^{ABI} = 30 + \sqrt{2E(W_T)} \quad (9)$$

$$K_{Jc}(med) = 30 + 70e^{0.019(T-T_0)} \quad \text{MPa}\sqrt{\text{m}} \quad (10)$$

$$K_{ld}(med) = 30 + 70e^{0.019(T-T_0+T_{shift})} \quad \text{MPa}\sqrt{\text{m}} \quad (11)$$

$$T_{shift}(^{\circ}F) = 215 - 1.5\sigma_y(ksi) \quad \text{for } 36 \text{ ksi} < \sigma_y < 140 \text{ ksi} \quad (12)$$

Table X2-1b – Definitions (Reference X2-2)

C_p	= true plastic strain,
d_p	= plastic indentation diameter,
D	= diameter of the ball indenter.
σ_t	= true stress,
P	= applied indentation load,
δ	= a parameter whose value depends on the stage of development of the plastic zone beneath the indenter.

h_t and d_t are the total indentation depth and total indentation diameter while the load is being applied, respectively.

A is the material yield parameter and m is Meyer's index.

σ_y is the ABI-determined yield strength, β_m is the material yield slope, and B is the yield-strength offset-constant.

The Indentation Deformation Energy (IDE) is a function of depth (h) and mean pressure (P_m)

The critical indentation depth (h_f) is the depth when the maximum stress equals the critical fracture stress of the ferritic steel at the low-test temperature.

The static fracture toughness, K_{Jc} , has a non-zero lower shelf even at very low-test temperatures.

The fracture toughness energy in J-Integral units is W .

W_o is the lower shelf energy per unit area (30 MPa \sqrt{m}).

W_T is the temperature-dependent energy ($W_T = IDE$).

T is the test temperature in °C and T_o is the reference temperature when $K_{Jc} = 100$ MPa \sqrt{m}

K_{Jd} is the median dynamic fracture toughness

X2.2.1 The Critical Fracture Stress (σ_f): The σ_f value as a function of test temperature was calculated using the semi-empirical Equation 4 and the fracture toughness and yield strength values of nuclear pressure vessel steel material from Oak Ridge National Laboratory. Using Equation 4 (given below) and the ORNL data produces the tabulated values of critical fracture stress as a function of test temperature shown in Table X2-2 and plotted in Figure X2-3.

$$\sigma_f = \sigma_y \left[1 + \ln \left(1 + 2360 \left(\frac{K_{Jc}}{\sigma_y} \right)^2 \right) \right] = 1.1 P_m \quad (4)$$

Where P_m is the mean pressure underneath the spherical indenter, “ln” is the natural logarithm, and K_{Jc} is the cleavage fracture toughness. The maximum stress ($1.1 P_m$) increases as the ABI depth increases and when it reaches the critical fracture stress value at the ABI test temperature before attaining a normalized depth of $d/D = 0.6$ (i.e., 12% strain), then the test is analyzed according to the critical fracture stress model and the concept of fracture toughness master curve is applicable where the reference temperature is determined from a minimum of 3 ABI tests. Numerous ABI tests conducted on various ferritic steels at low-test temperatures produced reference temperatures that are within 5°C from those determined from destructive fracture toughness specimens tested according to ASTM Standards E1820 and E1921.

X2.2.2 Critical Fracture Strain Model: If the maximum stress (equal to the critical fracture stress at the ABI test temperature) is not reached before a normalized indentation depth of $d/D = 0.6$ (i.e., 12% strain where “d” is the indentation chordal diameter on the sample surface and “D” is the indenter diameter),

then the test is analyzed using the critical fracture strain model by integrating the indentation deformation energy (mean pressure as a function of depth) up to an empirically conservative depth value of 12% strain. Since localized cooling of an ABI test area of an in-service structure (a pipeline or a storage tank, etc.) is not practical or safe, the reasonably conservative (within 10%) fracture toughness values obtained from a minimum of three ABI tests, analyzed using the critical fracture strain model, can be used to determine a very conservative reference temperature (up to 70C° higher than that if the critical fracture stress model was applied on samples tested at low temperatures).

X2.3 Examples of HTTM results (One lab ILS): Examples of the HTM-measured fracture toughness results on pipeline steel and on nuclear pressure vessel steel are shown in Figures X2-4 and X2-5.

Table X2-2 Critical Fracture Stress of Ferritic Steels as a Function of Test Temperature

Test Temperature, (°C)	Critical Fracture Stress, σ_f (MPa)	Test Temperature, (°F)	Critical Fracture Stress, σ_f (ksi)
-100	2275	-148	330
-90	2280	-130	331
-80	2295	-112	333
-70	2322	-94	337
-60	2363	-76	343
-50	2417	-58	351
-40	2488	-40	361
-30	2575	-22	373
-20	2680	-4	389
-10	2804	14	407
0	2949	32	428
10	3115	50	452
20	3304	68	479

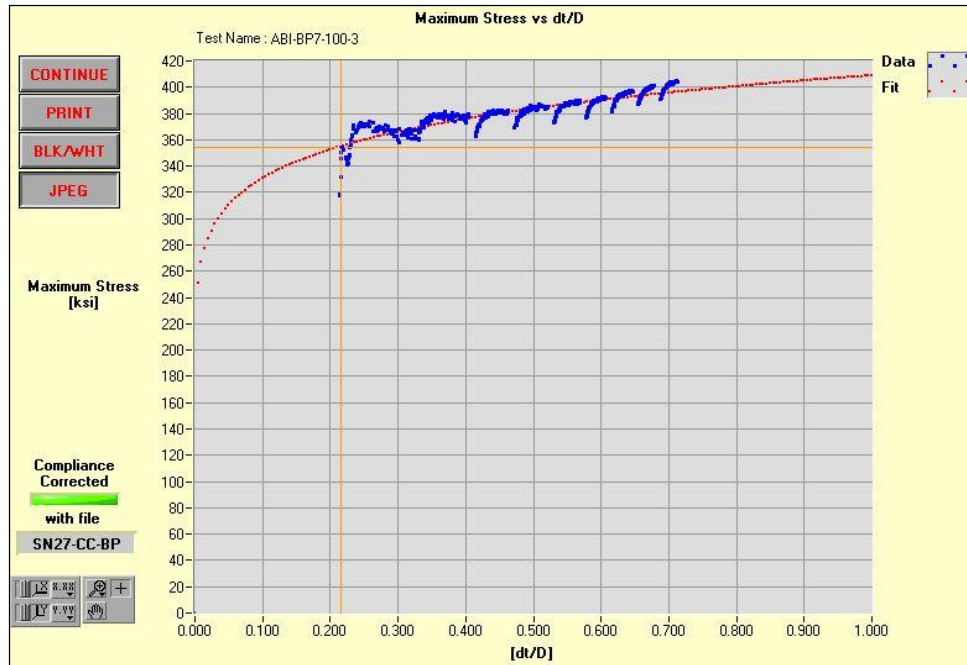


Fig. X2-1a Example of the use of the critical fracture stress model to determine the critical indentation depth (corresponding to the critical fracture stress at -100°C) in order to integrate the indentation deformation energy up to the critical depth to calculate fracture toughness from the multi-axis ABI test conducted here at -100°C on a BP steel from a storage tank.

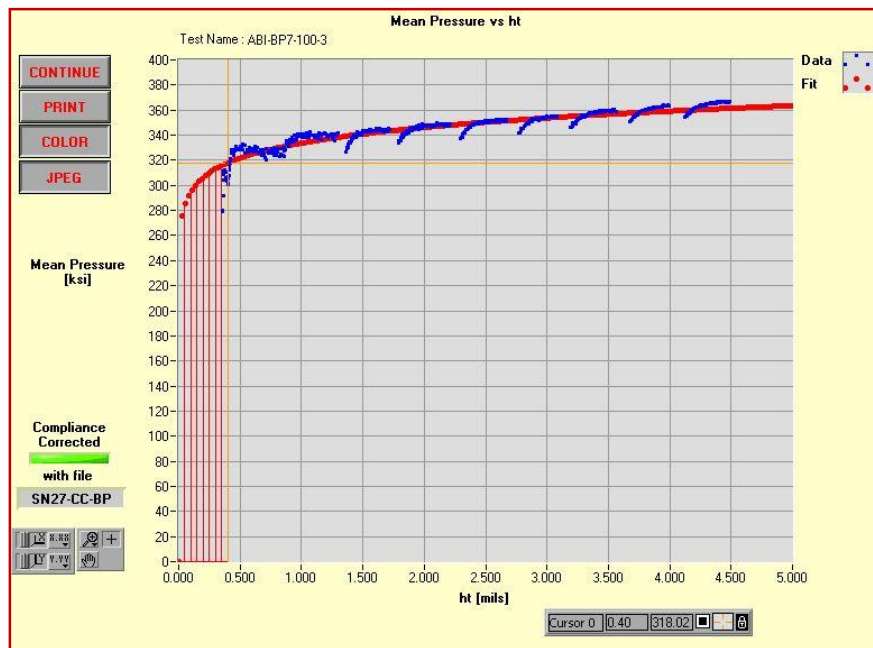


Fig. X2-1b Example of the use of the critical fracture stress model to determine the temperature-dependent part of the fracture toughness by integrating the deformation energy (mean pressure under the ball indenter) versus depth (corresponding to the critical fracture stress at -100°C shown above in Fig. X2-1a).

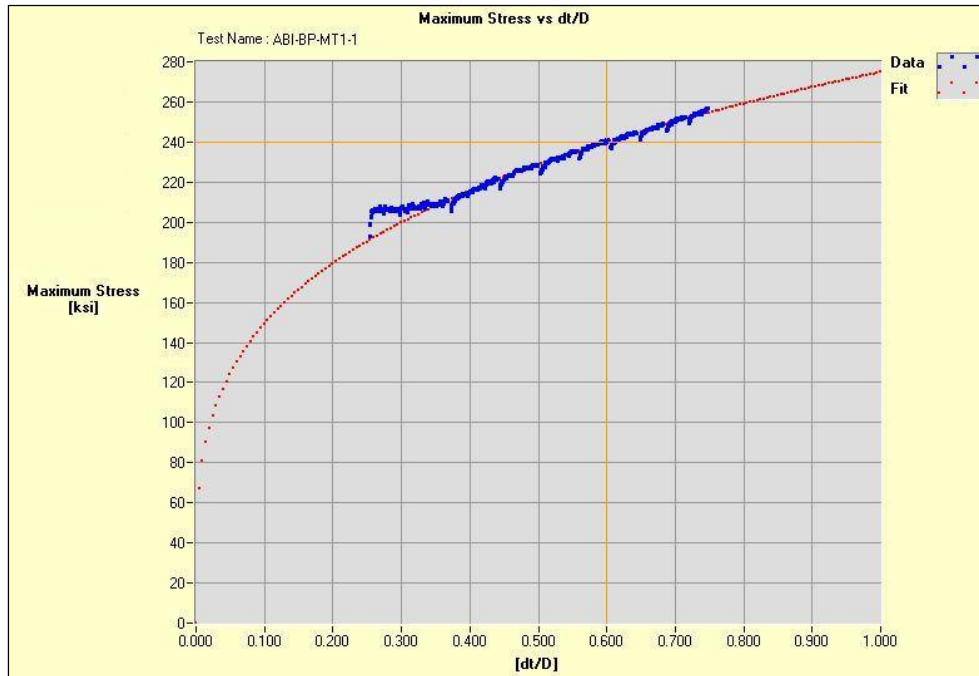


Fig. X2-2a Example of the use of the critical fracture strain model when testing a ductile material at room temperature where the critical fracture stress (479 ksi at 20°C) is not reached at a normalized depth of $d_t/D = 0.6$.

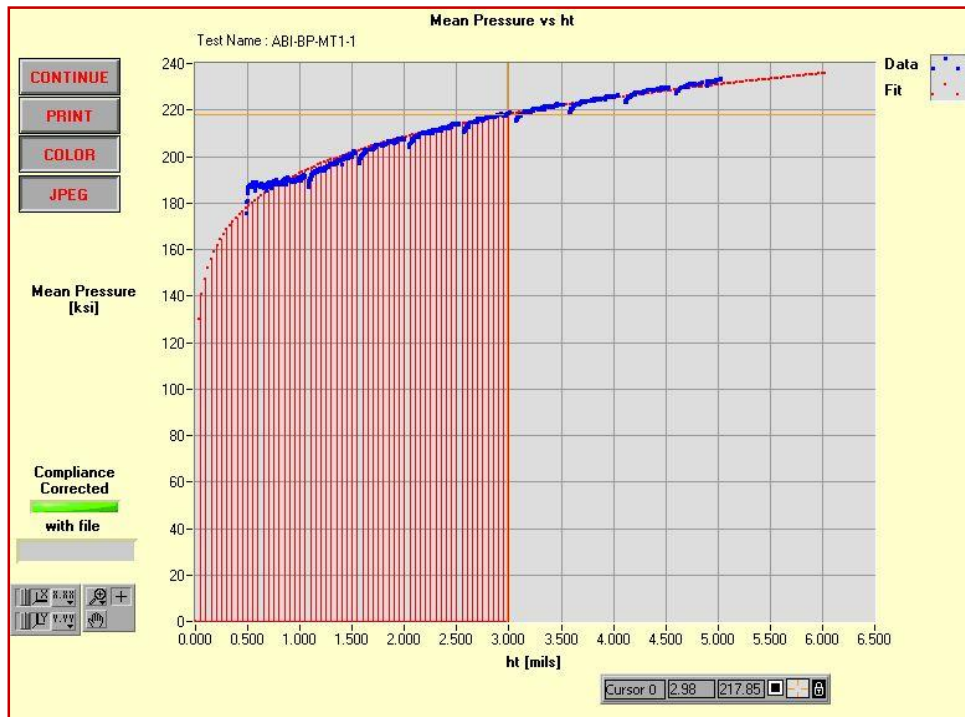


Fig. X2-2b Example of the use of the critical fracture strain model to determine the temperature-dependent part of the fracture toughness by integrating the deformation energy (mean pressure under the ball indenter) versus depth (corresponding to the critical fracture strain of 12% at $d_t/D = 0.6$ when testing a ductile material at room temperature as shown above in Fig. X2-2a).

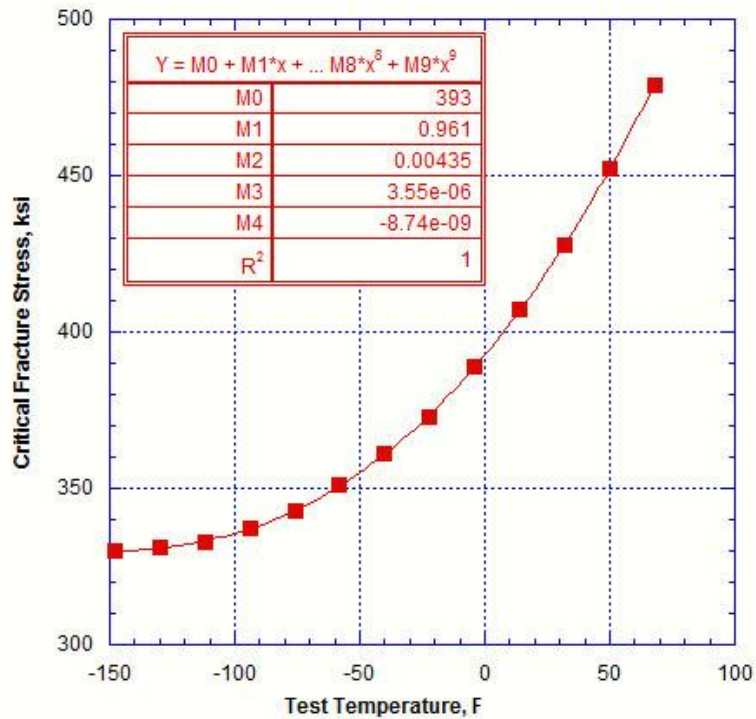
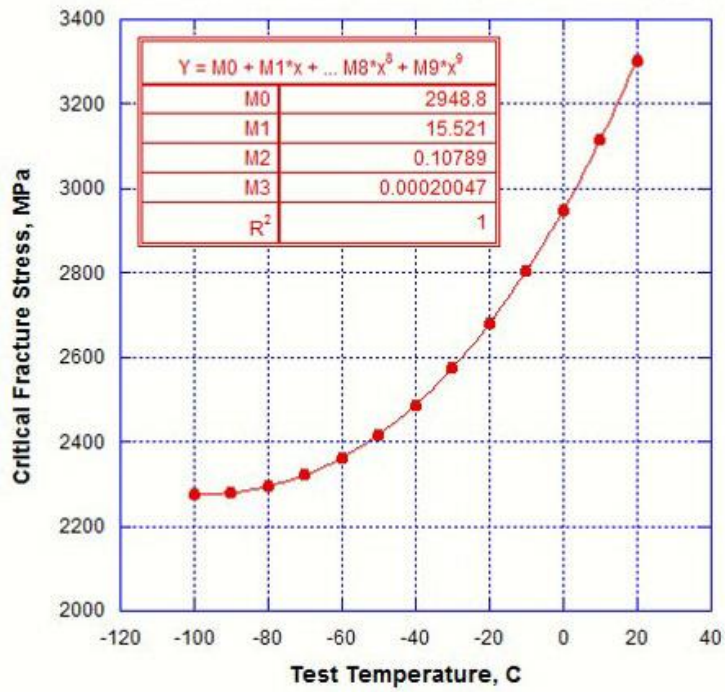
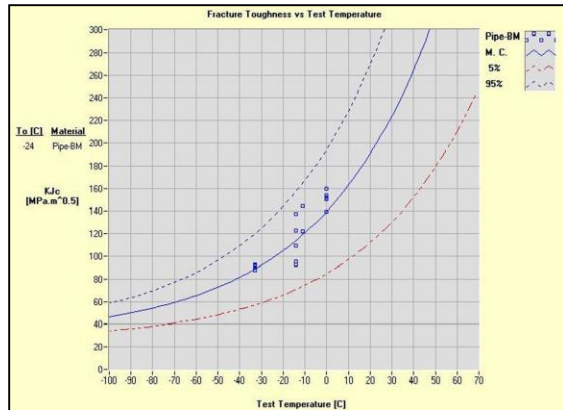
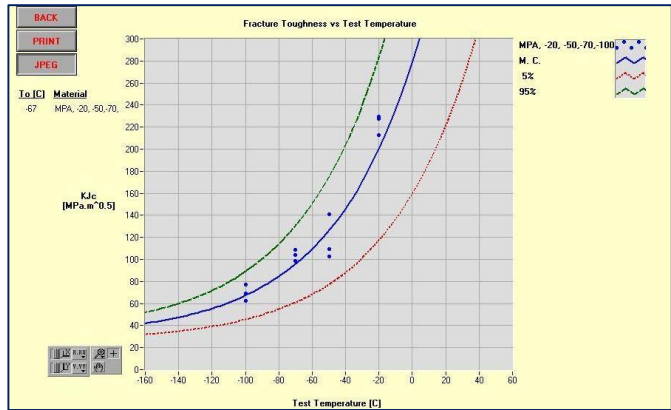


Fig. X2-3 Critical fracture stress (σ_f) versus test temperature calculated from Equation 4 above in SI and English units.

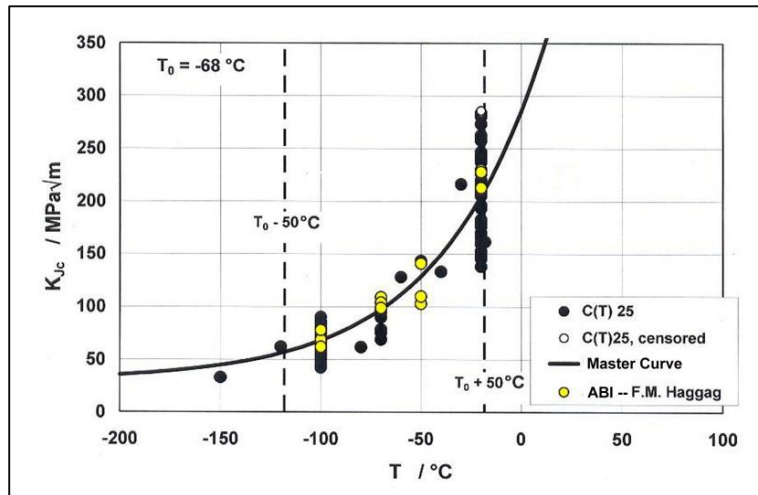


(a) Pipeline steel



(b) Nuclear Pressure Vessel steel

Fig. X2-4 Fracture toughness test results, their median master curves, and the 95% and 5% confidence curves.



(a)



(b)

Fig. X2-5 Comparison of the HTM/ABI-determined fracture toughness values (Yellow solid circles) and Reference Temperature (T_0) with those obtained from 100 25-mm-thick CT fracture toughness specimens (Black/dark circles, destructive tests were conducted at MPA, Germany, Ref. X2-7). The HTM-determined K_{Ic} results are shown by yellow/light solid circles. The Reference Temperature (T_0) of -68°C from destructive tests is in excellent agreement with the HTM- T_0 of -67°C (previous Fig. X2-4b, see the broken specimen photo on the right showing the HTM test locations at various test temperatures).

The average HTM-determined fracture toughness value from three room temperature tests on the nuclear pressure vessel sample of $221 \text{ MPa}\sqrt{\text{m}}$ was in good agreement with those from the destructive specimens with values ranging from $177 \text{ MPa}\sqrt{\text{m}}$ to $221 \text{ MPa}\sqrt{\text{m}}$. None of the room temperature test results from HTM tests could be included in the Master curve because the critical fracture stress was not achieved at room temperature.

X2-2.0 REFERENCES:

X2-1. Rolfe, Stanley T. and Barsom, John M., *Fracture and Fatigue Control in Structures: Applications of Fracture Mechanics*, Prentice-Hall, Inc., Englewood Cliffs, New Jersey, 1977, p. 129.

X2-2. Haggag, Fahmy M., “Indentation Technique Provides Pipeline Integrity Monitoring,” *Oil and Gas Journal*, August 14, 2006, p. 58-62.

X2-3. Haggag, F. M., “Nondestructive and Localized Measurements of Stress-Strain Curves and Fracture Toughness of Ferritic Steels at Various Temperatures Using Innovative Stress-Strain Microprobe™ Technology,” DOE-SBIR Phase II final report *DOE/ER/82115-2*, under grant number DE-FG02-96ER82115, 1999.

X2-4. Haggag, Fahmy M., 2002, “In-Service Nondestructive Measurements of Stress-Strain Curves and Fracture Toughness of Oil and Gas Pipelines: Examples of Fitness-for-Purpose Applications,” *Proceedings of the 5th International Conference on Pipeline Rehabilitation & Maintenance, Det Norske Veritas, Bahrain, Paper 7*.

X2-5. Haggag, Fahmy M. and Philips, Larry D., “Innovative Nondestructive Method Determines Fracture Toughness of In-Service Pipelines,” *ASME Proceedings of IPC 2004*, International Pipeline Conference, October 4-8, 2004, Calgary, Alberta, Canada, *IPC04-0345*, 2004.

X2-6. Haggag, Fahmy M., “In-Situ Measurement of Pipeline Mechanical Properties Using Stress-Strain Microprobe® – Validation of Data for Increased Confidence & Accuracy,” *PRCI Report L52280*, under Contract PR-345-063517, April 1, 2007.

X2-7. Haggag, Fahmy M., “Novel Localized Measurements of Fracture Toughness and Determination of the Reference Temperature of Ferritic Steels and Welds Using the ABI® Test Method,”

[https://www.researchgate.net/publication/283327046 Novel Localized Measurements of Fracture Toughness and Determination of the Reference Temperature of Ferritic Steels and Welds Using the ABI Test Method](https://www.researchgate.net/publication/283327046_Novel_Localized_Measurements_of_Fracture_Toughness_and_Determination_of_the_Reference_Temperature_of_Ferritic_Steels_and_Welds_Using_the_ABI_Test_Method)